Pure and Applied Mathematics Journal
2025, Vol. 14, No. 3, pp. 34-68
https://doi.org/10.11648/j.pamj.20251403.12

Research Article

Mapping the Geometric Structure of the Leech Lattice

Hal M. Switkay*

Department of Arts and Sciences, Goldey-Beacom College, Wilmington, USA

Abstract

The Leech lattice occupies a central place in exceptional mathematics and coding theory, but because it is 24-dimensional, its geometric structure is difficult to visualize. We elucidate a coordinate system employed in Conway's and Sloane's *Sphere Packings, Lattices and Groups* to describe and to illustrate the environs of the Leech lattice's deep holes but never explained in that book. By using this coordinate system for the deep holes, we are able to provide colorful diagrams for the environs of several deep holes. The most interesting of those deep holes is E_8^3, and we describe a new E_8^3-based coordinate system for the Leech lattice. We enumerate the Delaunay cells of the Leech lattice immediately neighboring a Delaunay cell of type E_8^3, neighboring in the sense of intersecting the latter cell in a 23-dimensional face. There are 729 such faces, but fewer isometry classes of neighboring cells, including both deep holes and shallow holes. We also enumerate the Delaunay cells of the Leech lattice in close proximity to a Delaunay cell of type E_8^3, close in the sense of having all vertices less than $\sqrt{2.2}$ distant from the center of E_8^3; the latter's circumradius is $\sqrt{2}$. Neither of the two classes of Delaunay cells enumerated below is a subset of the other. We next consider conjectures about the Leech lattice and the several lattices with similar properties, most especially the lattices $\mathbb{Z}$, A_2, $\mathbb{Z}^2$, D_4, and E_8. Other lattices sharing fewer optimality properties include the Coxeter-Todd lattice K_{12} and the Barnes-Wall lattice Λ_{16}. The properties of greatest interest are those involving various measures of high degrees of symmetry, as well as various measures of high efficiency in packing and covering. Our culminating theorem is a partial classification of lattices that have very strong properties similar to those of the Leech lattice.

Keywords

Leech Lattice, E8 Lattice, 24 Dimensions, Coxeter Diagram, Delaunay Cell

1. Introduction

In the preface to the first edition of J. H. Conway's and N. J. A. Sloane's *Sphere Packings, Lattices and Groups* [24], the following comments appear regarding the E_8 lattice and the Leech lattice Λ_{24}:"…[they] are unexpectedly good and very symmetrical packings, and have a number of remarkable and mysterious properties, not all of which are completely understood even today."[i] The paper [3] by R. E. Borcherds, one of the most elegant mathematical papers ever written, dispelled much of the mystery of the Leech lattice by unifying the treatment of its remarkable properties.

The Leech lattice occupies a central place in exceptional mathematics: the study of those objects that are the exceptions, or sporadic objects, in the many classification theorems of mathematics[ii]. Smaller exceptional objects have automorphism groups that are nearly always subquotients of $\cdot 0 \cong Co_0 \cong \mathrm{Aut}(\Lambda_{24})$, of order $8315553613086720000 = 2^{22} \times 3^9 \times 5^4 \times 7^2 \times 11 \times 13 \times 23$; while the largest finite exceptional object, the Monster simple group, of order

*Corresponding author: switkay@gbc.edu (Hal M. Switkay)

Received: 19 June 2025; **Accepted:** 9 July 2025; **Published:** 28 July 2025

$$808017424794512875886459904961710757005754368000000000 = -2^{46} \times 3^{20} \times 5^{9} \times 7^{6} \times 11^{2} \times 13^{3} \times 17 \times 19 \times 23 \times 29 \times 31 \times 41 \times 47 \times 59 \times 71$$

is constructed using Λ_{24}; see [24], chapter 29. (Twelve of the 26 exceptional finite simple groups are subquotients of $\mathrm{Aut}(\Lambda_{24})$; see [1]).

The Leech lattice plays an important role in error-correcting codes, among other areas. There appears to be considerable practical value to finding methods to visualize and navigate within the Leech lattice, ways that are easier than using a coordinate system of length 24. Such methods are developed in this paper.

2. The Deep Holes of the Leech Lattice

The list of Delaunay cells in the Leech lattice has been enumerated completely by R. E. Borcherds, J. H. Conway, and L. Queen; see [24], chapter 25. It includes 23 deep holes of circumradius $\sqrt{2}$, and 284 shallow holes of smaller circumradius. A deep (respectively, shallow) hole is a Delaunay cell whose circumradius equals (respectively, is less than) the covering radius of the lattice. We think of the Delaunay tessellation associated with a lattice as a sort of property map of the appropriate Euclidean space, in which the deep holes are mansions and the shallow holes are cottages. Each shallow hole, as well as two of the 23 deep holes (D_{24} and A_{24}), is a simplex. The remaining 21 deep holes are orthogonal sums of simplexes; and every 23-dimensional face of every hole is a simplex.

Various statistics may be computed regarding the 23 deep holes; see tables 1 and 2. In almost every respect, E_8^3 is the most important of the deep holes. A fuller understanding of its environs should make the Leech lattice more accessible for applications.[iii]

Among the statistics referred to above are popularity and diversity. The *popularity* of a Delaunay cell is proportional to the fraction of R^{24} (equivalently, of a Voronoi cell) occupied by cells of the given type, and is computed by dividing the volume of the given cell by the order of its automorphism group, g in table 1. (The quantity svol is introduced in [24], chapter 25, and stands for scaled volume; it is defined as the true volume times 24!, in order to make the results whole numbers.) The *diversity* of a Delaunay cell should be defined as the number of non-isometric Delaunay cells neighboring the given cell; because this is often tedious to determine in practice, we compute a smaller proxy for this number, defined as the number of faces of the given cell divided by the order of its automorphism group. We define two Delaunay cells as *neighbors* if their intersection is a 23-dimensional face of each.

E_8^3 is the most popular and the most diverse of all the 307 Delaunay cells; in fact, E_8^3 accounts for more than 6% of the total volume of R^{24} (equivalently, of a Voronoi cell). The second and third most popular and diverse Delaunay cells, $D_{10}E_7^2$ and $D_{16}E_8$, are full-fledged neighbors of E_8^3, and their three-way intersection is a 21-dimensional face of all three cells. The popularity and diversity of E_8^3 are consequences of the fact that E_8 is the only extended Coxeter-Dynkin diagram that has no non-trivial automorphisms.

Table 2 includes the total weight product for each deep hole. The *total weight product* is defined to be the product of the weights attached to each node of all the Coxeter-Dynkin diagrams for the hole.[iv] To compute the total weight product, we may multiply the following numbers together for each component of the hole diagram: for A_n, 1; for D_n, 2^{n-3}; for E_6, 24; for E_7, 288; and for E_8, 17280. The maximum weight product, 17280^3, occurs in the case of E_8^3. We will make extensive use of the weight product concept later in this paper, as a convenient measure of the proximity of two holes.[v]

There is a canonical set of vectors associated with each of the 23 deep holes that spans the Leech lattice. Referring to the "holy" constructions described in [24], chapter 24, the vectors in each spanning set take the form $f_i - g_w$, where f_i is a fundamental vector for the Niemeier lattice associated with the given deep hole and g_w is a glue vector. The cardinality of this spanning set equals the product of the number of fundamental vectors (24 plus the number of connected components in the diagram, or V in Table 2, because it represents the number of vertices of the deep hole) times the number of glue vectors ($|G_\infty|$ in table 2). This spanning set of vectors has smallest cardinality, 27, in the case of E_8^3, providing a far simpler spanning set than the set associated with the extended Golay binary code of length 24.

Tables 1 and 2 provide some of the basic statistics about the 23 deep holes, including the Coxeter number, *h*. Much of the information is taken from [24]. Decimals are rounded to a convenient precision. The E_8^3 coordinate system will be elucidated below.

Table 1. *Statistics of the deep holes in the Leech lattice (part 1).*

Deep hole (or Niemeier lattice)	Svol	g	Faces	Popularity = svol/g	Diversity = faces/g
E_8^3	27000	6	729	4500	121.5
$D_{16}E_8$	1800	2	153	900	76.5
$D_{10}E_7^2$	23328	8	704	2916	88

Deep hole (or Niemeier lattice)	Svol	g	Faces	Popularity = svol/g	Diversity = faces/g
D_8^3	21952	48	729	457.33333	15.1875
D_{24}	92	2	25	46	12.5
D_{12}^2	1936	8	169	242	21.125
$A_{17}E_7$	1944	12	144	162	12
$A_{11}D_7E_6$	20736	24	672	864	28
E_6^4	186624	432	2401	432	5.55787
A_8^3	19683	324	729	60.75	2.25
$A_{15}D_9$	2048	16	160	128	10
D_6^4	160000	384	2401	416.66667	6.252604
$A_7^2D_5^2$	131072	256	2304	512	9
A_{24}	125	10	25	12.5	2.5
$A_9^2D_6$	20000	80	700	250	8.75
A_4^6	1953125	30000	15625	65.104167	0.520833
A_{12}^2	2197	52	169	42.25	3.25
A_6^4	117649	1176	2401	100.04167	2.041667
$A_5^4D_4$	559872	3456	6480	162	1.875
D_4^6	2985984	138240	15625	21.6	0.113028
A_3^8	16777216	688128	65536	24.380952	0.095238
A_2^{12}	387420489	138568320	531441	2.7958807	0.003835
A_1^{24}	68719476736	1002795171840	16777216	0.0685279	0.0000167

Table 2. *Statistics of the deep holes in the Leech lattice (part 2).*

Deep hole (or Niemeier lattice)	Total weight product	V	$\|G_\infty\|$	$V \times \|G_\infty\|$	*h*	Weight product, closest approach to E_8^3	Largest dimension intersection with E_8^3	E_8^3 vertices not in intersection	Magnitude remotest vector, closest approach to E_8^3
E_8^3	5159780352000	27	1	27	30	1	24	∅	0
$D_{16}E_8$	141557760	26	2	52	30	4	23	e8;d8;d8	2
$D_{10}E_7^2$	10616832	27	4	108	18	8	23	e7a1;e7a1;d8	2
D_8^3	32768	27	8	216	14	8	23	d8;d8;d8	2
D_{24}	2097152	25	2	50	46	12	22	d8;a8;e8,d8	2
D_{12}^2	262144	26	4	104	22	16	22	d8;d5a3;e8,d8	2
$A_{17}E_7$	288	26	6	156	18	18	22	a8;a8;e8,e7a1	3
$A_{11}D_7E_6$	384	27	12	324	12	18	22	a8;e6a2;e8,d8	3
E_6^4	331776	28	9	252	18	27	23	e6a2;e6a2;e6a2	3
A_8^3	1	27	27	729	9	27	23	a8;a8;a8	3
$A_{15}D_9$	64	26	8	208	16	32	22	e8,d8;a7a1;a7a1	3
D_6^4	4096	28	16	448	10	64	21	d5a3;e7a1,d8;e7a1,d8	4

Deep hole (or Niemeier lattice)	**Total weight product**	**V**	**$\|G_\infty\|$**	**$V\times\|G_\infty\|$**	***h***	**Weight product, closest approach to E_8^3**	**Largest dimension intersection with E_8^3**	**E_8^3 vertices not in intersection**	**Magnitude remotest vector, closest approach to E_8^3**
$A_7^2D_5^2$	16	28	32	896	8	64	23	a7a1;a7a1;d5a3	4
A_{24}	1	25	5	125	25	72	21	a8;e8,a8;d8,a7a1	3
$A_9^2D_6$	8	27	20	540	10	100	21	e8,e7a1,d8;a4a4;a4a4	5
A_4^6	1	30	125	3750	5	125	23	a4a4;a4a4;a4a4	5
A_{12}^2	1	26	13	338	13	288	20	e8,a7a1;d8,a7a1;a8,e6a1	4
A_6^4	1	28	49	1372	7	?	?	?	?
$A_5^4D_4$	2	29	72	2088	6	?	?	?	?
D_4^6	64	30	64	1920	6	512	20	$(d8,d5a3)^3$	6
A_3^8	1	32	256	8192	4	6400	17	?	7
A_2^{12}	1	36	729	26244	3	5832	20	$(e6a2,a5a2a1)^3$	≥9
A_1^{24}	1	48	4096	196608	2	884736	14	$(e7a1,d8,d5a3,a5a2a1)^3$	≥10

Table 3 indicates which deep holes are neighbors of other deep holes; multiple neighbor relations are indicated by multiple check marks. This table is only known to be complete for deep hole neighbors of E_8^3; in particular, we expect more deep hole neighbor relations for $D_{10}E_7^2$ and $D_{16}E_8$. $\{E_8^3,\ D_{16}E_8,\ D_{10}E_7^2,\ D_8^3\}$ forms a maximal set of holes that are mutually neighbors, as does $\{D_{16}E_8,\ D_{10}E_7^2,\ D_8^3,\ D_{12}^2\}$. Table 4 provides a partial list of the intersections for neighboring deep holes. These relations are easy to verify; deep holes X and Y are neighbors only if one can remove one node from each connected component of X and from each connected component of Y, with the result being two isomorphic graphs on 24 nodes that are unions of finite-type Coxeter-Dynkin diagrams (thus representing a 23-dimensional simplex, a face of each deep hole). The converse need not be true. For example, D_6^4 and D_4^6 appear not to be neighbors, despite the fact that both have faces of the form $d_4^4a_1^8$; this simply means that the automorphism group of the Leech lattice is not transitive on all the instances of every graph we are interested in. We employ the [24] convention under which finite-type (spherical) diagrams are identified by lowercase letters, and extended (Euclidean) diagrams are identified by capital letters. Some of the neighbor relations are visible in figure 2. Among the deep hole neighbors of E_8^3 are numerous other copies of E_8^3, as well as 7 other non-isometric deep holes, more than any other deep hole.

Table 3. *Neighbor relations among the deep holes in the Leech lattice.*

E_8^3	**$D_{16}E_8$**	**$D_{10}E_7^2$**	**D_8^3**	**D_{24}**	**D_{12}^2**	**$A_{17}E_7$**	**$A_{11}D_7E_6$**	**E_6^4**	**A_8^3**	**$A_{15}D_9$**	**D_6^4**	**$A_7^2D_5^2$**	**A_{24}**	**$A_9^2D_6$**	**A_4^6**	**A_{12}^2**	**A_6^4**	**$A_5^4D_4$**	**D_4^6**	**A_3^8**	**A_2^{12}**	**A_1^{24}**	
✓✓✓ ✓✓✓ ✓✓✓ ✓✓✓	✓	✓✓ ✓✓	✓✓ ✓					✓✓ ✓	✓			✓			✓								E_8^3
		✓	✓	✓	✓																		$D_{16}E_8$
			✓		✓						✓	✓											$D_{10}E_7^2$
					✓						✓								✓				D_8^3
					✓																		D_{24}
											✓												D_{12}^2

E_8^3	$D_{16}E_8$	$D_{10}E_7^2$	D_8^3	D_{24}	D_{12}^2	$A_{17}E_7$	$A_{11}D_7E_6$	E_6^4	A_8^3	$A_{15}D_9$	D_6^4	$A_7^2D_5^2$	A_{24}	$A_9^2D_6$	A_4^6	A_{12}^2	A_6^4	$A_5^4D_4$	D_4^6	A_3^8	A_2^{12}	A_1^{24}	
																							$A_{17}E_7$
																							$A_{11}D_7E_6$
																		✓			✓		E_6^4
																							A_8^3
																							$A_{15}D_9$
																				✓			D_6^4
																							$A_7^2D_5^2$
																							A_{24}
																							$A_9^2D_6$
																							A_4^6
																							A_{12}^2
																							A_6^4
																							$A_5^4D_4$
																			✓			✓	D_4^6
																							A_3^8
																							A_2^{12}
																							A_1^{24}

Table 4. *Sample intersections of neighboring deep holes.*

Deep hole	Deep hole	Intersections
E_8^3	E_8^3	$d_8e_6^2a_2^2$ | $a_8^2e_6a_2$ | $e_7e_6a_5a_2^2a_1^2$ | $d_8a_7^2a_1^2$ | $e_6d_5^2a_3^2a_1$ | $d_8a_4^4$
		$a_7d_5^2a_3^2a_1$ | $e_6a_4^4a_2$ | $d_5^2a_4^2a_3^2$ | $a_8a_5^2a_2^2a_1^2$ | $d_5a_5^2a_3a_2^2a_1^2$ | $a_5^2a_4^2a_2^2a_1^2$
E_8^3	$D_{16}E_8$	$e_8d_8^2$
E_8^3	$D_{10}E_7^2$	$d_8e_7^2a_1^2$ | $e_7d_5^2a_3^2a_1$ | $d_8a_5^2a_2^2a_1^2$ | $d_5^2a_5a_3^2a_2a_1$
E_8^3	D_8^3	d_8^3 | $d_8d_5^2a_3^2$ | $d_5^3a_3^3$
E_8^3	E_6^4	$e_6^3a_2^3$ | $e_6a_5^2a_2^3a_1^2$ | $a_5^3a_2^3a_1^3$
E_8^3	A_8^3	a_8^3
E_8^3	$A_7^2D_5^2$	$a_7^2d_5a_3a_1^2$
E_8^3	A_4^6	a_4^6
$D_{16}E_8$	$D_{10}E_7^2$	$d_{10}e_7d_6a_1$
$D_{16}E_8$	D_8^3	d_8^3
$D_{16}E_8$	D_{24}	$d_{16}d_8$
$D_{16}E_8$	D_{12}^2	$d_{12}d_8d_4$

Deep hole	Deep hole	Intersections
$D_{10}E_7^2$	D_8^3	$d_8d_6^2a_1^4$
$D_{10}E_7^2$	D_{12}^2	$d_{10}d_6^2a_1^2$
$D_{10}E_7^2$	D_6^4	$d_6^3d_4a_1^2$
$D_{10}E_7^2$	$A_7^2D_5^2$	$a_7^2d_5^2$
D_8^3	D_{12}^2	$d_8^2d_4^2$
D_8^3	D_6^4	$d_6^2d_4^2a_1^4$
D_8^3	D_4^6	d_4^6
D_{24}	D_{12}^2	d_{12}^2
D_{12}^2	D_6^4	d_6^4
E_6^4	$A_5^4D_4$	$a_5^4a_1^4$
E_6^4	A_2^{12}	a_2^{12}
D_6^4	A_3^8	a_3^8
D_4^6	D_4^6	$d_4^2a_1^{16}$
D_4^6	A_1^{24}	a_1^{24}

An energetic reader may choose to determine all maximal intersections of pairs of deep holes. All 23 deep hole diagrams contain subgraphs of the form a_1^{12}. Use caution; although $\cdot\infty \cong Co_\infty \cong Aut_\infty(\Lambda_{24})$, the full automorphism group of the Leech lattice (including translations), is transitive on graphs of the form a_1^5, it fails to be transitive on graphs of the form a_1^6, let alone a_1^{12}.[vi]

3. Visualizing the Leech Lattice

As discussed in chapter 27 of [24], the Leech lattice has the structure of a graph if we place $(d-4)/2$ edges between two distinct lattice elements whose squared distance is d. Thus lattice elements at minimal squared distance 4 are not joined, and lattice elements at squared distance 6 are joined by a single edge. The whole Leech lattice may be seen as a graph with infinitely many nodes, and automorphism group $\cdot\infty \cong Co_\infty \cong Aut_\infty(\Lambda_{24})$. Each node is not joined with precisely 196560 other nodes; is singly-joined with 16773120 other nodes; is doubly-joined with 398034000 other nodes; etc.[vii] It turns out that the subgraph associated with the vertices of any of the 23 deep holes is in fact the extended or affine Coxeter-Dynkin diagram associated with that root system; see [24], chapters 23 and 24, as well as [3]. [3] contains an elegant proof that the deep holes of the Leech lattice are in one-to-one correspondence with the 23 Niemeier lattices (even self-dual 24-dimensional lattices) of minimal norm 2. B. B. Venkov proves in [24], chapter 18, that the Niemeier lattices of minimal norm 2 are in turn in one-to-one correspondence with the 23 root systems of total rank 24 and constant Coxeter number h. This explains the extent of the first column of table 1.

Diagrams of the vicinity of the A_{24} deep hole are drawn in [24], chapters 25 and 27. The vicinity of the E_8^3 deep hole is shown in figure 1.[viii] All vectors are shown whose squared distance from the center of the hole is no more than 2.2. The convex hull of these 37 vectors includes 12 of the 23 deep holes in their entirety, as well as glue vectors for each of the 12, and thus a large cohort of shallow holes; the deep holes and shallow holes referenced above comprise more than 90% of the volume of R^{24} (equivalently, of a Voronoi cell)[ix]; and the convex hull of these 37 vectors contains the centers of 8 more deep holes (the centers of only A_1^{24}, A_2^{12}, and A_3^8 are missing). Indeed, one can see much of the A_n-tree and much of the D_n-tree from chapter 23 of [24]. The method of constructing the graph shown in figure 1 is described in a later section, after we have constructed an E_8^3-based coordinate system for the Leech lattice.

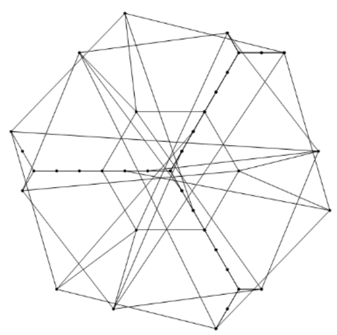

Figure 1. *The environs of the E_8^3 deep hole.*

The image in figure 1 was created in 2007, based on a prototype created in 2006 and an earlier hand-drawn version dating to 2002. In 2008, this image was used to illustrate a webpage on the BBC website [2] advertising an interview with Marcus du Sautoy. The latter was invited to discuss his book *Symmetry* [13], culminating in a discussion of the Monster simple group. As noted earlier, the Monster is usually constructed by making use of the Leech lattice (see [24], chapter 29), and diagrams like those in figures 1-5 provide the only means known to date, other than section or projection, to visualize the shape of portions of the Leech lattice.

4. Navigating the Leech lattice

The environs of the deep holes are described in [24], chapters 23 and 24. As mentioned above, every deep hole has circumradius $\sqrt{2}$ when the minimal norm is 4 (making the packing radius equal to 1). The lattice elements at squared distance 2 from the center of the deep hole, namely the vertices of that Delaunay cell, are the V fundamental vectors, whose graph is the extended Coxeter-Dynkin diagram associated with that hole, and the 23 types listed in table 1 occur uniquely up to isometry of the Leech lattice; see [24], chapter 23. Proceeding outward from the center of the deep hole, the next shell of vectors encountered is the set of $|G_\infty|$ glue vectors, at squared distance $2 + 2/h$ from the center of the deep hole. Graphically, each glue vector is joined by one edge to a node of weight 1 (an extending node) in each of the components of the hole's graph. This is established in [24], chapter 24.

Beyond this point, additional vectors are described by the "starry" coordinate system, related to the author orally [10], based on the "holy" constructions of [24], chapter 24. Fix a deep hole, with Coxeter number h. All Leech lattice vectors have a magnitude with respect to the hole, a magnitude that assumes all whole number values. A vector of *magnitude m* has squared distance $2 + 2m/h$ from the hole's center; so as in astronomy, a higher magnitude star is dimmer and more distant. Thus the hole vertices (fundamental vectors) are the brightest stars, with magnitude 0, and the glue vectors have magnitude 1. A vector v of magnitude m is joined m-fold to each of the connected components of the hole diagram, in the following sense: m is equal to the sum of all products of the form (weight of fundamental vector f) times (number of edges connecting f and v), such sums taking place within each connected component of the hole diagram.

Let X be the name of a deep hole, and n be a whole number. Define $X + n$ to be the set of Leech lattice vectors which are stars of magnitude no more than n with respect to X. $X + (n + 1)$ does not contain every possible graphical extension of $X + n$, restricted solely by the conditions above. Rather, the larger graph must satisfy additional conditions enumerated in [24], chapter 23, culminating in the complete enumeration of Delaunay cells in [24], chapter 25. Briefly, the graph of every Delaunay cell can be one of only two types: 1) a disjoint union of extended Coxeter-Dynkin diagrams of constant Coxeter number and total rank 24 (the 23 deep holes); or 2) a disjoint union of finite-type Coxeter-Dynkin diagrams of total rank 25 (the 284 shallow holes, all simplexes). In particular, no extended Coxeter-Dynkin diagram is permitted unless it is a component of one of the 23 combinations listed in table 1.

With the "starry" coordinate system in hand, it is easy to produce diagrams of the environs of any of the deep holes. Some of these are depicted in figure 2, shown against the background of figure 1, to allow an easy comparison of location.[x] Black nodes are hole vertices (fundamental vectors), red nodes are glue vectors (stars of magnitude 1), orange nodes are stars of magnitude 2, green nodes are stars of magnitude 3, blue nodes are stars of magnitude 4, and purple nodes are stars of magnitude 5. Edges connecting two nodes are given the color of the larger magnitude star. Our goal is to draw all Leech lattice vectors whose squared distance from selected deep hole centers is no more than $2\frac{2}{9}$, except that in cases where the glue vectors are too numerous, we draw $X + *$, indicating the hole vertices together with a subset of the glue vectors. We are confident that the drawings are in fact complete for Leech lattice vectors whose squared distance from the chosen deep hole centers is less than $2\frac{2}{13}$. The graph of $A_{24} + 2$ appearing in figure 2 is isomorphic to the aforementioned graph of the vicinity of A_{24} appearing in chapters 25 and 27 of [24]. The [24] depiction of this graph is more attractive than the one in figure 2, because it displays that deep hole's automorphism group, the dihedral group of order 10. Similar aesthetic improvements could be made to the other graphs, but for our purposes, it is preferable to display all deep holes against the same background, namely, $E_8^3 + 3$. Only one representative of any orbit under $Aut(E_8^3)$ is shown.

The method of constructing these graphs is described below. Together, these diagrams constitute an atlas of the majority of the Leech lattice's 307 Delaunay cells (23 deep holes plus 284 shallow holes), accounting for the vast majority of the volume of R^{24} (equivalently, of a Voronoi cell); in fact, the Delaunay cells included in the convex hull of $E_8^3 + 3$ alone constitute about 90.92% of the volume of R^{24}. Those deep holes not shown in figure 2 have small Coxeter number, large volume, large glue code, large automorphism group, and most importantly, low popularity and diversity; consequently, the list of neighbors for such deep holes is short, and not difficult to enumerate. This atlas could be completed by drawing diagrams for the remaining deep holes together with just one glue vector, on the conjecture that every shallow hole is a *close neighbor* of some deep hole X, in the sense that the two cells are neighbors (sharing a 23-dimensional face), and the shallow hole is a subset of $X + 1$.

In figure 2, three parameters are described for each hole: wp is the weight product of the E_8^3 nodes not in the intersection of the given cell with the central E_8^3; dim is the dimension of the intersection of the given cell with the central E_8^3; and mag is the magnitude of the cell vertex most remote from the central E_8^3. E_8^3 is depicted in more than one position, reflecting its high popularity.

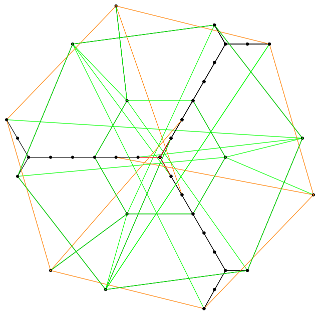

E_8^3+3: wp 1, dim 24, mag 0

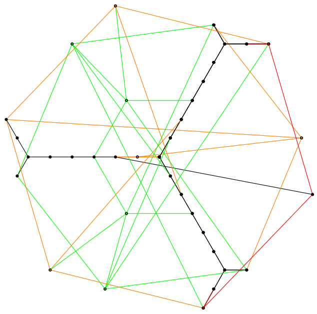

$D_{16}E_8+3$: wp 4, dim 23, mag 2

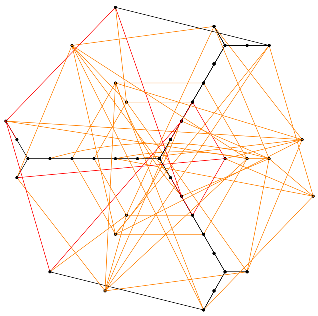

$D_{10}E_7^2+2$: wp 8, dim 23, mag 2

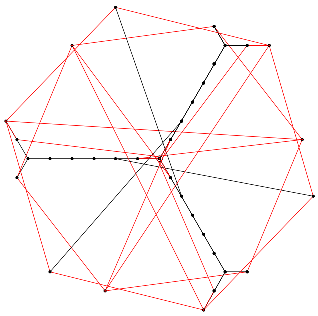

D_8^3+1: wp 8, dim 23, mag 2

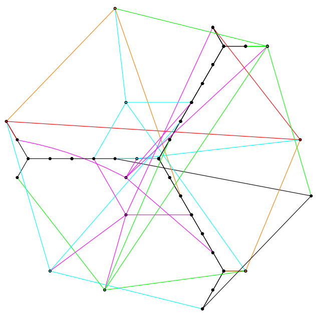

$D_{24}+5$: wp 12, dim 22, mag 2

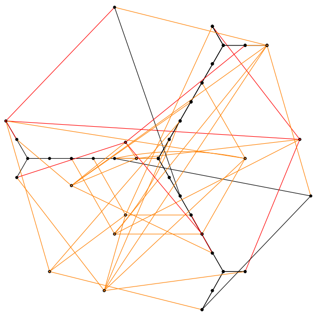

D_{12}^2+2: wp 16, dim 22, mag 2

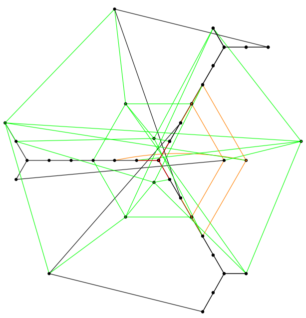

E_8^3+3: wp 18, dim 23, mag 3

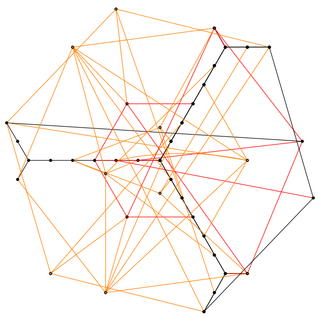

$A_{17}E_7+2$: wp 18, dim 22, mag 3

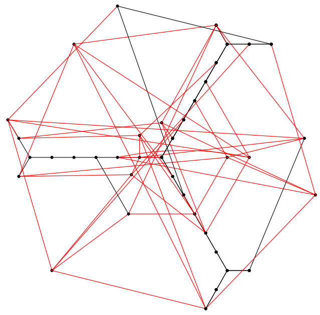

$A_{11}D_7E_6+1$: wp 18, dim 22, mag 3

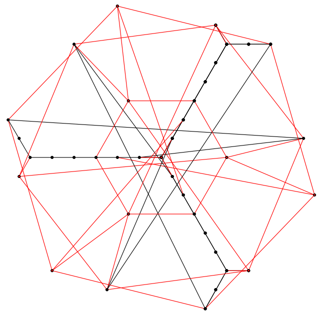

A_8^3+*: wp 27, dim 23, mag 3

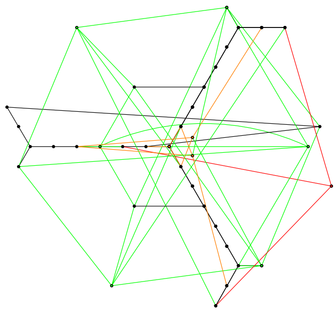

E_8^3+3: wp 27, dim 23, mag 3

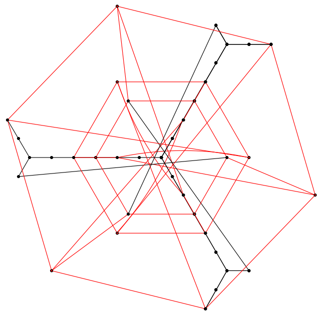

E_6^4+1: wp 27, dim 23, mag 3

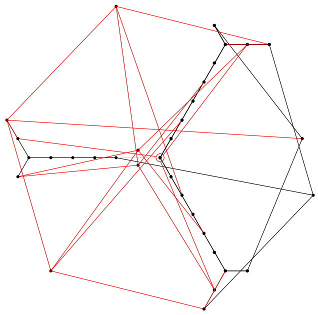

$A_{15}D_9+1$: wp 32, dim 22, mag 3

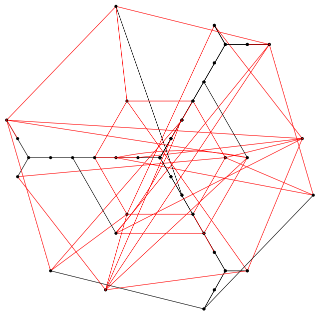

D_6^4+*: wp 64, dim 21, mag 4

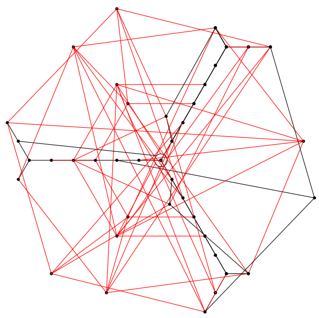

$A_7^2D_5^2+*$: wp 64, dim 23, mag 4

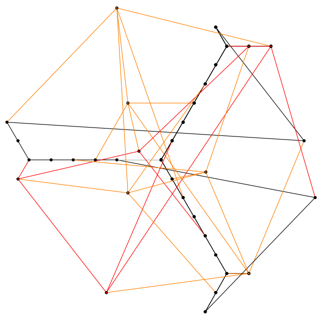

$A_{24}+2$: wp 72, dim 21, mag 3

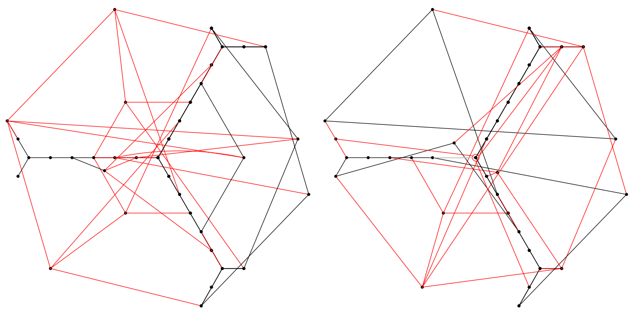

Figure 2. *The environs of some deep holes.*

5. An E_8^3-Based Coordinate System for the Leech Lattice

We provide names for the nodes in a Coxeter-Dynkin diagram, whether of finite (spherical) type or extended (Euclidean) type. Every such node may be named by the graph that results from its removal from the original graph. This naming scheme does not usually provide unique names for the nodes of Coxeter-Dynkin diagrams, which almost always have non-trivial graph automorphisms. The only exceptions are the graphs a_1, e_7, e_8, and E_8. Under this convention, the nodes along the spine of the latter are named e8, e7a1, e6a2, d5a3, a4a4, a5a2a1, a7a1, and d8; the additional node is named a8.[xi] A labeled E_8 diagram is depicted in figure 3, with the numbers in parentheses being the weights of the nodes.[xii] The coloring scheme for the labels is a reminder of the coloring scheme for the stars, although all the nodes depicted in figure 3 are fundamental vectors, and hence magnitude 0 stars, for an E_8^3 hole.

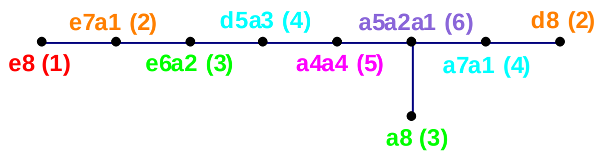

Figure 3. *A labeled* E_8 *diagram.*

The naming convention described above lays the basis for an E_8^3-based coordinate system for the Leech lattice, centered at a deep hole of type E_8^3. There are three coordinates, and any point in R^{24} may be identified with three coordinates that have magnitude m, where $m \geq -30$ (in general, for analogous coordinate systems based at other deep holes, $m \geq -h$, where h is the deep hole's Coxeter number); the resulting point has magnitude m.

The center of the E_8^3 hole, although not a lattice vector, has magnitude -30, not far distant from the astronomical magnitude of the sun; and in the analogous coordinate system based on any other deep hole, its center would have magnitude -*h*, where *h* is the hole's Coxeter number. The precise coordinates of the center of the E_8^3 hole are:

(-e8-e7a1-d8-a8-e6a2-a7a1-d5a3-a4a4-a5a2a1,
-e8-e7a1-d8-a8-e6a2-a7a1-d5a3-a4a4-a5a2a1,
-e8-e7a1-d8-a8-e6a2-a7a1-d5a3-a4a4-a5a2a1).

The terms are arranged in descending order of the orders of the corresponding Weyl groups, but this is not essential.

The fundamental vectors, or cell vertices, have magnitude 0. For example, one of these vertices, an extending node of one of the E_8 diagrams, has coordinates (-2e8+e7a1,0,0). The sole glue vector, with magnitude 1, has coordinates (e8,e8,e8). The three stars of magnitude 2 have coordinates that are permutations of (d8,d8,e7a1). There are two orbits of three magnitude 3 stars, with coordinates that are permutations of (e6a2,e6a2,a8) and (a8,a8,e8+d8). These assertions will be justified below.

In table 5, we provide coordinates for Leech lattice vectors in the first few shells around a deep hole of type E_8^3. All permutations of the three coordinates are permitted. We are confident that the list is complete up to and including magnitude 3; beyond this point, we name only those vectors that are vertices of cells listed in table 5, or that are vertices of other nearby deep holes or are low magnitude stars thereof. We can also discover stars by applying isometries of nearby holes to known stars. For example, D_8^3 and A_8^3 are neighbors of E_8^3; each of the former has non-trivial isometries that act similarly on each of its components without permuting the components. The components of A_8^3 are enneagons, visible in figure 2, sharing 8 vertices each with neighboring E_8 diagrams; one fruitful *autometry*[xiii] of the Leech lattice involves rotating each enneagon component 3 places in the same direction, and in fact, this is how some of the entries in table 3 were discovered. There are autometries of the A_8^3 and D_8^3 holes with similar actions; in the context of the former, each enneagon undergoes a reflection, fixing only the d5a3 node, approximately reversing the order of the nodes along the spine of each E_8 diagram. Combining this autometry with the previously mentioned rotation, we get a symmetric group of degree 3 and order 6. These autometries commute with the permutations of the three coordinates, yielding a subgroup with structure $Sym_3 \times Sym_3$ within $Aut(\Lambda_{24})$.

Table 5. *Some Leech lattice vectors in the vicinity of* E_8^3.

Magnitude	Number of vectors of this type	E_8^3 coordinates	Fundamental vector name	Fundamental vector weight
0	3	(-2e8+e7a1,0,0)	e8	1

Magnitude	Number of vectors of this type	$E_8{}^3$ coordinates	Fundamental vector name	Fundamental vector weight
0	3	(e8-2e7a1+e6a2,0,0)	e7a1	2
0	3	(-2d8+a7a1,0,0)	d8	2
0	3	(-2a8+a5a2a1,0,0)	a8	3
0	3	(e7a1-2e6a2+d5a3,0,0)	e6a2	3
0	3	(d8-2a7a1+a5a2a1,0,0)	a7a1	4
0	3	(e6a2-2d5a3+a4a4,0,0)	d5a3	4
0	3	(d5a3-2a4a4+a5a2a1,0,0)	a4a4	5
0	3	(a8+a7a1+a4a4-2a5a2a1,0,0)	a5a2a1	6
1	1	(e8,e8,e8)		
2	3	(d8,d8,e7a1)		
3	3	(e6a2,e6a2,a8)		
3	3	(a8,a8,e8+d8)		
4	1	(a7a1,a7a1,a7a1)		
4	1	(d5a3,d5a3,d5a3)		
4	3	(d5a3,d5a3,e7a1+d8)		
4	3	(a7a1,a7a1,d5a3)		
4	6	(d5a3,a7a1,e8+a8)		
5	3	(a4a4,a4a4,e8+d5a3)		
5	3	(a4a4,a4a4,d8+a8)		
5	3	(a4a4,e7a1+a8,e7a1+a8)		
6	3	(a5a2a1,a5a2a1,a8+e6a2)		
6	3	(a5a2a1,d8+d5a3,d8+d5a3)		

With our coordinate systems in hand, we can describe how to construct graphs of the vicinity of any deep hole, and therefore the way to discover the existence of the stars enumerated in table 3. We will focus on E_8^3, making use of figure 4. Figure 4 contains the same nodes and edges as figure 1, colored to show magnitudes; a smaller version is the initial diagram in figure 2.

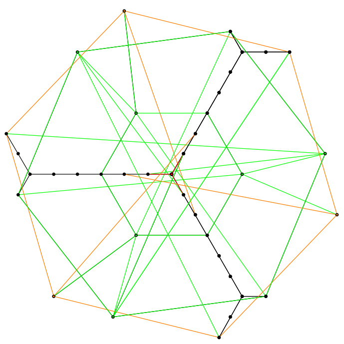

Figure 4. *Stars of magnitude at most 3 in the vicinity of* E_8^3.

The Leech lattice contains, uniquely up to isometry, deep holes corresponding to all configurations of extended Coxeter-Dynkin diagrams with constant Coxeter number h and total rank 24. In particular, there is a unique deep hole of type E_8^3; these are the nodes and edges shown in black in figure 4. We also know the glue code has order 1, so there is a unique glue vector, shown in red, and it must be singly-joined to the unique extending node in each component; these are the red edges. This process can be carried out in theory for any of the 23 deep holes, but is only feasible in practice for deep holes with small glue codes (that is, with $|G_\infty|$ small).

Next, examine the 28-node graph $E_8^3 + 1$ consisting of the black and red nodes and edges in figure 4. This graph includes various extended Coxeter-Dynkin diagrams: namely, D_{16}, D_{10}, E_6, E_7, and a new E_8. Focus first on the D_{16} subgraph. By virtue of [24], chapter 23, we know that any D_{16} diagram is associated with a unique deep hole of the form $D_{16}E_8$. The portion of $E_8^3 + 1$ that is completely disjoined from D_{16} is an e_8 diagram. In other words, $E_8^3 + 1$ contains a subgraph of the form $D_{16}e_8$. This must be contained in a unique $D_{16}E_8$.

But e_8 can only be extended to E_8 in one way. Thus, there must exist a new, as yet undetected Leech lattice vector, which is joined singly to the node known as e7a1 in the extended diagram. This new vector has magnitude 2 with respect to E_8^3. Conveniently, it may be singly-joined to the d8 nodes in the other E_8 components, which are not contained in the D_{16} subgraph of E_8^3+1, yielding a vector with coordinates (d8,d8,e7a1). Symmetries of the E_8^3 hole reveal two other magnitude 2 stars, for a total of three. They are shown in orange in figure 4.

We could have proceeded to examine the portion of E_8^3+1 disjoined from the D_{10} diagram, and discovered that E_8^3+1 includes a subgraph of the form $D_{10}e_7^2$. Every D_{10} diagram is associated with a unique deep hole of the form $D_{10}E_7^2$. Analogously, $D_{10}e_7^2$ can be extended to $D_{10}E_7^2$ in only one way. The new nodes extending the e_7 diagrams must be attached to the nodes known as d8 within the E_8 diagrams, and thus have magnitude 2. In fact, these stars are precisely the same discovered above starting with D_{16}.

We discover two orbits of three stars each of magnitude 3, shown in green in figure 4. One is discovered by considering the diagram $E_6e_6^3$ as a subgraph of E_8^3+1; this can be extended only to E_6^4 and not to $A_{11}D_7E_6$. The new magnitude 3 stars have coordinates (e6a2,e6a2,a8) and its permutations. The other orbit is discovered by considering the diagram a_8^3 as a subgraph of E_8^3, but this argument is not as obvious; a_8^3 does also appear as a subgraph of the diagram for the shallow hole $a_8^3a_1$. Because of this uncertainty, and the question of joins between new nodes being added to the graph, we pause and change direction temporarily.

Contemplating our larger 31-node graph E_8^3+2, consisting of the black, red, and orange nodes and edges in figure 4, we now see within it six deep holes: not just the E_8^3, $D_{16}E_8$, and $D_{10}E_7^2$ holes identified earlier, but also D_{24}, D_{12}^2, and D_8^3. We also see the following components of other deep holes: A_5, A_{11}, A_{17}, D_5, D_6, and D_9. The new deep holes are shown in figure 2, all against the backdrop of the original E_8^3. All these deep holes have glue vectors of their own. The glue codes are described in detail by Venkov in [24], chapter 18, and in particular we know the distance between glue vectors. For all deep holes except A_1^{24}, A_2^{12}, and A_3^8, the squared distance between distinct glue vectors is either 4 or 6, so that the graph restricted to the glue vectors alone is an ordinary graph with no multiply-joined edges.

To illustrate, let us contrast $D_{16}E_8$ with D_{24}. Both have glue codes of order 2. The difference is that the glue vectors of the former are at squared distance 4, whereas the glue vectors of the latter at squared distance 6. Thus the glue vectors of $D_{16}E_8$ are not joined by an edge, but the glue vectors of D_{24} are joined by an edge. By drawing all of our diagrams consistently against the background of E_8^3, we enable information about low-magnitude stars of one deep hole to inform us about relations among larger-magnitude stars of another nearby deep hole. We also take advantage of the automorphism groups of the nearby deep holes, not merely the E_8^3 hole, to locate additional nodes and edges. This bootstrapping process was employed to build the diagrams in figure 2.

We now return to the question of additional stars of magnitude 3. Within the graph E_8^3+2, we observe a subgraph of the form $A_{17}e_7$. Any diagram of the form A_{17} must be contained in a unique $A_{17}E_7$, and $A_{17}e_7$ can only be extended to $A_{17}E_7$ in one way. The new vectors have coordinates (a8,a8,e8+d8) and its permutations.

Joins between newly discovered stars can be determined in various ways. Sometimes a newly discovered star creates a cycle within the enlarged graph, a cycle that forms a forbidden A_n; this is a signal that the new vector must be joined to a previously known vector. Also, as part of the bootstrapping process, when we discover a deep hole Y in the environs of a deep hole X, it is likely we will find some, and sometimes all, of the glue vectors of Y nearby as well, and the graphical structure of $Y+1$ is completely determined from [24], chapters 18, 23 and 24. For example, within E_8^3+2, we espy $D_{16}E_8+1$. Within E_8^3+3, we can see $D_{10}E_7^2+1$ and $D_{24}+1$. The latter includes A_{24} as a subgraph, and soon we are discovering its own glue vectors, etc., etc., and so on and so forth![xiv]

The graph formed by the glue vectors associated with a deep hole is an interesting graph. We identify the graphs associated with glue codes of small order in table 6. For these 11 deep holes, but for none of the others, the glue code graph is a union of Coxeter-Dynkin diagrams of finite (spherical) type or of extended (Euclidean) type. The structure of the 23 glue codes is elucidated by Venkov, in chapter 18 of [24].[xv] The glue vectors have the shape of a regular simplex in just five cases: E_8^3, $D_{16}E_8$, D_{24}, $D_{10}E_7^2$, and E_6^4.

Table 6. *Glue code graphs.*

Deep hole	Glue code G_∞	Glue code graph
E_8^3	1	a_1
$D_{16}E_8$	2	a_1^2
D_{24}	2	a_2
$D_{10}E_7^2$	2^2	a_1^4
D_{12}^2	2^2	a_2^2
A_{24}	5	A_4
$A_{17}E_7$	6	a_2^3
D_8^3	2^3	a_2^4
$A_{15}D_9$	8	A_7
E_6^4	3^2	a_1^9
$A_{11}D_7E_6$	12	A_{11}

6. Neighbors of E_8^3

It is now time to enumerate the Delaunay cells in the vicinity of the E_8^3 deep hole. We determine distance from the E_8^3 deep hole by three criteria: 1) the dimension of the intersection of the Delaunay cell with E_8^3 (larger is closer); 2) the distance of the most remote point of the Delaunay cell from the center of E_8^3 (smaller is closer); and 3) the product of the weights of those nodes of E_8^3 that do not belong to the Delaunay cell (smaller is closer).

We aim to provide a combined complete list of 1) the 729 neighbors of E_8^3 (cells for which the intersection dimension is 23) as well as 2) the cells, the magnitude of whose most remote vertex with respect to E_8^3 is no more than 2 (that is, the cells that are included in $E_8^3 + 2$). Neither of these classes is a subset of the other. The first goal is accomplished by removing any one of the nine vertices in each of the three connected components of the E_8^3 diagram (this can happen, of course, in $9^3 = 729$ ways), and adding new nodes, stars of minimal magnitude with respect to E_8^3, from figure 1 or figure 2 (when the magnitude of the most remote vector is no more than 3). These 729 cells fall into 165 orbits under the action of $Aut(E_8^3)$. The second goal is accomplished by seeking all subsets of $E_8^3 + 2$ (the 27 black nodes, 1 red node, and 3 orange nodes in the E_8^3+3 diagram in figure 2) that satisfy the restrictions on Leech lattice Delaunay cells described above.

Note that the cells included in $E_8^3 + 1$ are either the central deep hole E_8^3 itself, or else 51 isometry classes of shallow holes that are neighbors of E_8^3. This follows from an examination of the 28-node graph $E_8^3 + 1$, which has the structure of a tree, uniquely among the 23 diagrams of the form $X + 1$.

The Delaunay cells in the vicinity of E_8^3 are listed in table 7, listed in increasing order of weight product with respect to E_8^3. For a neighbor of E_8^3, this weight product must lie between 1 and 216 inclusive; non-neighbors can have weight products as high as (and dividing) 17280^3, the total weight product of E_8^3. The cells are grouped by orbit under the action of the automorphism group of the E_8^3 hole (the group is the symmetric group of degree 3 and order 6). Each orbit contains either 1, 3, or 6 cells. Cells from classes 1 (the neighbors of E_8^3) and 2 (cells included in $E_8^3 + 2$) above are listed. We also list other cells of interest, such as deep holes with low weight product with respect to E_8^3, as well as *sticky holes*: the close neighbors of deep holes that result from removing the extending nodes that connect to a glue vector (so that the sticky hole for $A_{11}D_7E_6$ would be $a_{11}d_7e_6a_1$). The sticky holes for both $D_{10}E_7^2$ and $D_{16}E_8$ are themselves close neighbors of E_8^3, and the sticky hole for E_8^3 is in turn a close neighbor of both $D_{10}E_7^2$ and $D_{16}E_8$, reinforcing the mutual proximity of the most popular and diverse holes. The 25 neighbors of the sticky hole for E_8^3, namely $e_8^3a_1$, are, other than E_8^3 itself, all close neighbors of E_8^3.

Table 7. *Delaunay cells in the vicinity of E_8^3.*

Weight product	Intersection dimension	E_8^3 vertices not in intersection	Delaunay cells	Number of cells in this orbit	Magnitude of most remote vertex	Notes
1	24	∅	E_8^3	1	0	the central deep hole itself
1	23	e8; e8; e8	$e_8^3a_1$	1	1	close neighbor, sticky for E_8^3; smallest Delaunay cell
2	23	e8; e8; e7a1	$e_8^2e_7a_2$	3	1	close neighbor
2	23	e8; e8; d8	$d_9\ e_8^2$	3	1	close neighbor
3	23	e8; e8; a8	$a_9\ e_8^2$	3	1	close neighbor
3	23	e8; e8; e6a2	$e_8^2e_6a_3$	3	1	close neighbor
4	23	e8; e8; a7a1	$e_8^2a_8a_1$	3	1	close neighbor
4	23	e8; e8; d5a3	$e_8^2d_5a_4$	3	1	close neighbor
4	23	e8; e7a1; e7a1	$e_8e_7^2a_3$	3	1	close neighbor
4	23	e8; e7a1; d8	$d_{10}\ e_8e_7$	6	1	close neighbor
4	23	e8; d8; d8	$D_{16}E_8$	3	2	deep hole neighbor
5	23	e8; e8; a4a4	$e_8^2a_5a_4$	3	1	close neighbor
6	23	e8; e8; a5a2a1	$e_8^2a_6a_2a_1$	3	1	close neighbor
6	23	e8; e7a1; a8	$a_{10}e_8e_7$	6	1	close neighbor
6	23	e8; e7a1; e6a2	$e_8e_7e_6a_4$	6	1	close neighbor

Weight product	Intersection dimension	E_8^3 vertices not in intersection	Delaunay cells	Number of cells in this orbit	Magnitude of most remote vertex	Notes
6	23	e8; d8; a8	$d_{17}e_8$	6	1	close neighbor
6	23	e8; d8; e6a2	$d_{11}e_8e_6$	6	1	close neighbor
8	23	e8; e7a1; a7a1	$a_9e_8e_7a_1$	6	1	close neighbor
8	23	e8; e7a1; d5a3	$e_8e_7d_5a_5$	6	1	close neighbor
8	23	e8; d8; a7a1	$d_{16}e_8a_1$	6	1	close neighbor, sticky for $D_{16}E_8$
8	23	e8; d8; d5a3	$d_{12}e_8d_5$	6	1	close neighbor
8	23	e7a1; e7a1; e7a1	$e_7^3d_4$	1	1	close neighbor
8	23	e7a1; e7a1; d8	$D_{10}E_7^2$	3	2	deep hole neighbor
8	23	e7a1; d8; d8	$d_8^2e_7a_1a_1$	3	2	neighbor
8	23	d8; d8; d8	D_8^3	1	2	deep hole neighbor
8	20	e8, d8; e8, d8; e8, d8	$d_8^3a_1$	1	2	sticky for D_8^3
9	23	e8; a8; a8	$a_{17}e_8$	3	1	close neighbor
9	23	e8; a8; e6a2	$a_{11}e_8e_6$	6	1	close neighbor
9	23	e8; e6a2; e6a2	$e_8e_6^2a_5$	3	1	close neighbor
10	23	e8; e7a1; a4a4	$e_8e_7a_6a_4$	6	1	close neighbor
10	23	e8; d8; a4a4	$d_{13}e_8a_4$	6	1	close neighbor
12	23	e8; e7a1; a5a2a1	$e_8e_7a_7a_2a_1$	6	1	close neighbor
12	23	e8; d8; a5a2a1	$d_{14}e_8a_2a_1$	6	1	close neighbor
12	23	e8; a8; a7a1	$a_{16}e_8a_1$	6	1	close neighbor
12	23	e8; a8; d5a3	$a_{12}e_8d_5$	6	1	close neighbor
12	23	e8; e6a2; a7a1	$a_{10}e_8e_6a_1$	6	1	close neighbor
12	23	e8; e6a2; d5a3	$e_8e_6a_6d_5$	6	1	close neighbor
12	23	e7a1; e7a1; a8	$d_{11}e_7^2$	3	1	close neighbor
12	23	e7a1; e7a1; e6a2	$e_7^2e_6d_5$	3	1	close neighbor
12	23	e7a1; d8; a8	$a_9d_8e_7a_1$	6	2	neighbor
12	23	e7a1; d8; e6a2	$d_8e_7^2a_2a_1$	6	2	neighbor
12	23	d8; d8; a8	$d_9d_8^2$	3	2	neighbor
12	23	d8; d8; e6a2	$d_8^2e_6a_3$	3	2	neighbor
12	22	d8; a8; e8, d8	D_{24}	6	2	deep hole
12	22	e8, e7a1; d8; a8	$d_{18}e_7$	6	2	
12	22	e8, d8; e7a1; a8	$d_{18}e_7$	6	2	
12	21	d8; e8, d8; e8, a8	$d_{16}d_9$	6	2	
12	22	d8; e6a2; e8, e7a1	$d_{11}e_7^2$	6	2	
15	23	e8; a8; a4a4	$a_{13}e_8a_4$	6	1	close neighbor
15	23	e8; e6a2; a4a4	$e_8a_7e_6a_4$	6	1	close neighbor
16	23	e8; a7a1; a7a1	$a_{15}e_8a_1^2$	3	1	close neighbor
16	23	e8; a7a1; d5a3	$a_{11}e_8d_5a_1$	6	1	close neighbor

Weight product	**Intersection dimension**	**E_8^3 vertices not in intersection**	**Delaunay cells**	**Number of cells in this orbit**	**Magnitude of most remote vertex**	**Notes**
16	23	e8; d5a3; d5a3	$e_8a_7d_5^2$	3	1	close neighbor
16	23	e7a1; e7a1; a7a1	$d_{10}e_7^2a_1$	3	1	close neighbor, sticky for $D_{10}E_7^2$
16	23	e7a1; e7a1; d5a3	$e_7^2d_6d_5$	3	1	close neighbor
16	23	e7a1; d8; a7a1	$d_8e_7a_7a_2a_1$	6	2	neighbor
16	23	e7a1; d8; d5a3	$d_8e_7d_6a_3a_1$	6	2	neighbor
16	23	d8; d8; a7a1	$d_8^3a_1$	3	2	neighbor, sticky for D_8^3
16	23	d8; d8; d5a3	$d_8^2d_5d_4$	3	2	neighbor
16	22	d8; d5a3; e8, d8	D_{12}^2	6	2	deep hole
16	22	d8; e8, d8; a7a1	$d_{16}d_9$	6	2	
16	22	d8; e8, e7a1; a7a1	$d_{16}e_7a_2$	6	2	
16	22	d8; e8, d8; a7a1	$a_{16}d_9$	6	2	
16	22	e7a1; d8; e8, a7a1	$d_{10}e_7a_6a_2$	6	2	
18	23	e8; a8; a5a2a1	$a_{14}e_8a_2a_1$	6	1	close neighbor
18	23	e8; e6a2; a5a2a1	$e_8a_8e_6a_2a_1$	6	1	close neighbor
18	23	e7a1; a8; a8	$a_{17}e_7a_1$	3	2	neighbor, sticky for $A_{17}E_7$
18	23	e7a1; a8; e6a2	$e_8a_8e_6a_2a_1$	6	3	neighbor
18	23	e7a1; e6a2; e6a2	$e_7e_6^3$	3	1	close neighbor
18	23	d8; a8; a8	$d_9a_8^2$	3	3	neighbor
18	23	d8; a8; e6a2	$a_{11}d_8e_6$	6	2	neighbor
18	23	d8; e6a2; e6a2	E_8^3	3	3	deep hole neighbor
18	22	e8, e7a1; a8; a8	$A_{17}E_7$	3	3	deep hole
18	22	e8, d8; a8; e6a2	$A_{11}D_7E_6$	6	3	deep hole
18	22	e8, d8; a8; a8	d_{25}	6	2	
18	22	d8; a8; e8, a8	d_{25}	6	2	
18	22	e8, d8; a8; e6; a2	$d_{19}e_6$	6	2	
18	22	d8; a8; e8, e6a2	$d_{19}e_6$	6	2	
18	22	e7a1; a8; e8, a8	$a_{18}e_7$	6	2	
18	22	e8, e7a1; a8; a8	$a_{18}e_7$	6	2	
18	20	e8, d8; e8, e6a2; e8, e6a2	$e_8^3a_1$	3	3	sticky for E_8^3
20	23	e8; a7a1; a4a4	$a_{12}e_8a_4a_1$	6	1	close neighbor
20	23	e8; d5a3; a4a4	$e_8a_8d_5a_4$	6	1	close neighbor
20	23	e7a1; e7a1; a4a4	$e_7^2d_7a_4$	3	1	close neighbor
20	23	e7a1; d8; a4a4	$d_8e_7a_5a_4a_1$	6	2	neighbor
20	23	d8; d8; a4a4	$d_8^2d_5a_4$	3	2	neighbor
20	22	d8; e8, d8; a4a4	$d_{13}d_{12}$	6	2	
20	22	d8; e8, e7a1; a4a4	$d_{13}e_7a_5$	6	2	
24	23	e8; a7a1; a5a2a1	$a_{13}e_8a_2a_1a_1$	6	1	close neighbor

Weight product	Intersection dimension	E_8^3 vertices not in intersection	Delaunay cells	Number of cells in this orbit	Magnitude of most remote vertex	Notes
24	23	e8; d5a3; a5a2a1	$a_9e_8d_5a_2a_1$	6	1	close neighbor
24	23	e7a1; e7a1; a5a2a1	$d_8e_7^2a_2a_1$	3	1	close neighbor
24	23	e7a1; d8; a5a2a1	$d_8e_7a_5a_3a_1a_1$	6	2	neighbor
24	23	d8; d8; a5a2a1	$d_8^2d_6a_2a_1$	3	2	neighbor
24	23	e7a1; a8; a7a1	$a_{11}e_7a_5a_1^2$	6	2	neighbor
24	23	e7a1; a8; d5a3	$d_{14}e_7a_3a_1$	6	2	neighbor
24	23	e7a1; e6a2; a7a1	$e_8e_7a_7a_2a_1$	6	2	neighbor
24	23	e7a1; e6a2; d5a3	$e_7^2e_6d_5$	6	1	close neighbor
24	23	d8; a8; a7a1	$d_{16}a_8a_1$	6	3	neighbor
24	23	d8; a8; d5a3	$d_{12}d_8d_5$	6	2	neighbor
24	23	d8; e6a2; a7a1	$d_8a_7e_6a_4$	6	2	neighbor
24	23	d8; e6a2; d5a3	$d_8^2e_6a_3$	6	2	neighbor
24	22	e8, d8; a8; a7a1	$d_{24}a_1$	6	2	sticky for D_{24}
24	22	e8, a7a1; d8; a8	$d_{24}a_1$	6	2	sticky for D_{24}
24	22	e8, d8; a8; d5a3	$d_{20}d_5$	6	2	
24	22	d8; a8; e8, d5a3	$d_{20}d_5$	6	2	
24	22	d8; e8, d8; a5a2a1	$d_{14}d_{10}a_1$	6	2	
24	21	d8; e8, d8; e7a1, a8	$d_{14}d_{10}a_1$	6	2	
24	22	d8; a7a1; e8, a8	$d_{16}a_9$	6	2	
24	22	d8; a7a1; e8, e6a2	$d_{16}e_6a_3$	6	2	
24	22	d8; e6a2; e8, e7a1	$d_{12}d_7e_6$	6	2	
24	22	d8; d5a3; e8, e6a2	$d_{12}d_7e_6$	6	2	
24	22	d8; e8, e7a1; a5a2a1	$d_{14}e_7a_3a_1$	6	2	
24	22	d8; e8, d8; a5a2a1	$d_{10}d_8d_6a_1$	6	2	
24	21	d8; e8, a8; e7a1, d8	$d_{10}a_9d_6$	6	2	
25	23	e8; a4a4; a4a4	$a_9e_8a_4^2$	3	1	close neighbor
27	23	a8; a8; a8	A_8^3	1	3	deep hole neighbor
27	23	a8; a8; e6a2	E_8^3	3	3	deep hole neighbor
27	23	a8; e6a2; e6a2	$a_8e_6^2a_2^2a_1$	3	3	neighbor
27	23	e6a2; e6a2; e6a2	E_6^4	1	3	deep hole neighbor
30	23	e8; a4a4; a5a2a1	$a_{10}e_8a_4a_2a_1$	6	1	close neighbor
30	23	e7a1; a8; a4a4	$a_{13}e_7a_4a_1$	6	2	neighbor
30	23	e7a1; e6a2; a4a4	$e_8e_7e_6a_4$	6	1	close neighbor
30	23	d8; a8; a4a4	$d_{13}a_8a_4$	6	3	neighbor
30	23	d8; e6a2; a4a4	$d_8a_7e_6a_4$	6	2	neighbor
30	22	e8, d8; a8; a4a4	$d_{21}a_4$	6	2	
30	22	d8; a8; e8, a4a4	$d_{21}a_4$	6	2	
30	22	d8; e8, a8; a4a4	$d_{13}a_{12}$	6	2	

Weight product	Intersection dimension	E_8^3 vertices not in intersection	Delaunay cells	Number of cells in this orbit	Magnitude of most remote vertex	Notes
30	22	d8; e8, e6a2; a4a4	$d_{13}e_6a_6$	6	2	
32	23	e7a1; a7a1; a7a1	$e_7a_7^2a_3a_1$	3	2	neighbor
32	23	e7a1; a7a1; d5a3	$e_7d_7a_7a_3a_1$	6	2	neighbor
32	23	e7a1; d5a3; d5a3	$D_{10}E_7^2$	3	4	deep hole neighbor
32	23	d8; a7a1; a7a1	E_8^3	3	4	deep hole neighbor
32	23	d8; a7a1; d5a3	$d_8a_7d_5^2$	6	2	neighbor
32	23	d8; d5a3; d5a3	D_8^3	3	4	deep hole neighbor
32	22	e8, d8; a7a1; a7a1	$A_{15}D_9$	3	3	deep hole
32	22	d8; a7a1; e8, a7a1	$d_{16}a_8a_1$	6	2	
32	22	d8; a7a1; e8, d5a3	$d_{16}d_5a_4$	6	2	
32	22	e7a1; a7a1; e7a1, d8	$d_{10}e_7d_6a_2$	6	2	
32	22	e8, e7a1; a7a1; a7a1	$a_{15}e_7a_3$	3	2	
32	22	e7a1; d5a3; e7a1, d8	$e_7d_6^3$	6	2	
36	23	e8; a5a2a1; a5a2a1	$a_{11}e_8a_2^2a_1^2$	3	1	close neighbor
36	23	e7a1; a8; a5a2a1	$a_{11}e_7a_5a_1^2$	6	2	neighbor
36	23	e7a1; e6a2; a5a2a1	E_8^3	6	3	deep hole neighbor
36	23	d8; a8; a5a2a1	$d_{10}a_8a_5a_2$	6	3	neighbor
36	23	d8; e6a2; a5a2a1	$d_8e_6a_5^2a_1$	6	2	neighbor
36	23	a8; a8; a7a1	$a_9a_8^2$	3	3	neighbor
36	23	a8; a8; d5a3	$d_9a_8^2$	3	3	neighbor
36	23	a8; e6a2; a7a1	$e_8a_8e_6a_2a_1$	6	3	neighbor
36	23	a8; e6a2; d5a3	$a_8e_6d_5a_4a_2$	6	3	neighbor
36	23	e6a2; e6a2; a7a1	$a_8e_6^2a_2^2a_1$	3	3	neighbor
36	23	e6a2; e6a2; d5a3	$e_6^3a_3a_2^2$	3	3	neighbor
36	21	d8; e8, d8; a8, e6a2	$d_{13}d_{12}$	6	2	
36	22	e8, d8; a8; a5a2a1	$d_{22}a_2a_1$	6	2	
36	22	d8; a8; e8, a5a2a1	$d_{22}a_2a_1$	6	2	
36	21	d8; e6a2; e8, e7a1, d8	$d_{12}e_7d_6$	6	2	
36	22	a8; a8; e8, a7a1	$a_{24}a_1$	6	2	
36	22	a8; a7a1; e8, a8	$a_{24}a_1$	6	2	
36	22	d8; e8, a8; e7a1, a8	$a_{15}d_{10}$	6	2	
36	22	d8; e8, a8; a5a2a1	$d_{14}a_{10}a_1$	6	2	
36	22	d8; e8, e6a2; a5a2a1	$d_{14}e_6a_4a_1$	6	2	
40	23	e7a1; a7a1; a4a4	$e_7a_7a_6a_4a_1$	6	2	neighbor
40	23	e7a1; d5a3; a4a4	$d_{10}e_7a_4a_3a_1$	6	2	neighbor
40	23	d8; a7a1; a4a4	$d_8a_7e_6a_4$	6	2	neighbor
40	23	d8; d5a3; a4a4	$d_8^2d_5a_4$	6	2	neighbor
40	21	e8, d8; e7a1, d8; a4a4	$d_{12}e_7d_6$	6	2	

Weight product	Intersection dimension	E_8^3 vertices not in intersection	Delaunay cells	Number of cells in this orbit	Magnitude of most remote vertex	Notes
40	22	d8; a4a4; e8, a7a1	$d_{13}a_{11}a_1$	6	2	
40	22	d8; a7a1; e8, a4a4	$d_{16}a_5a_4$	6	2	
40	22	d8; a4a4; e8, d5a3	$d_{13}a_7d_5$	6	2	
45	23	a8; a8; a4a4	$a_9a_8^2$	3	3	neighbor
45	23	a8; e6a2; a4a4	$a_8e_6d_5a_4a_2$	6	3	neighbor
45	23	e6a2; e6a2; a4a4	$e_6^2a_5a_4a_2^2$	3	3	neighbor
48	23	e7a1; a7a1; a5a2a1	$e_7a_7a_5a_4a_1a_1$	6	2	neighbor
48	23	e7a1; d5a3; a5a2a1	$d_8e_7a_5a_3a_1a_1$	6	2	neighbor
48	23	d8; a7a1; a5a2a1	$d_8e_7a_7a_2a_1$	6	2	neighbor
48	23	d8; d5a3; a5a2a1	$d_8d_6d_5a_5a_1$	6	2	neighbor
48	23	a8; a7a1; a7a1	$d_9a_7^2a_1^2$	3	4	neighbor
48	23	a8; a7a1; d5a3	$a_9a_7d_5a_3a_1$	6	4	neighbor
48	23	a8; d5a3; d5a3	$a_8a_7d_5^2$	3	3	neighbor
48	23	e6a2; a7a1; a7a1	$a_7^2e_6d_5$	3	2	neighbor
48	23	e6a2; a7a1; d5a3	$a_{11}e_6d_5a_2a_1$	6	3	neighbor
48	23	e6a2; d5a3; d5a3	E_8^3	3	4	deep hole neighbor
48	22	e7a1; a7a1; e7a1, a8	$d_{10}a_8e_7$	6	2	
48	21	d8; e8, d8; e6a2, a7a1	$d_{12}d_9a_4$	6	2	
48	22	d8; a7a1; e8, a5a2a1	$d_{16}a_6a_2a_1$	6	2	
48	22	d8; e8, a7a1; a5a2a1	$d_{14}a_9a_1a_1$	6	2	
50	23	e7a1; a4a4; a4a4	$a_9e_7a_4^2a_1$	3	2	neighbor
50	23	d8; a4a4; a4a4	E_8^3	3	5	deep hole neighbor
54	23	a8; a8; a5a2a1	$a_8^3a_1$	3	3	neighbor
54	23	a8; e6a2; a5a2a1	$a_8e_6^2a_2^2a_1$	6	3	neighbor
54	23	e6a2; e6a2; a5a2a1	$e_6^2a_5a_2^4$	3	3	neighbor
60	23	e7a1; a4a4; a5a2a1	$e_7a_7a_5a_4a_1a_1$	6	2	neighbor
60	23	d8; a4a4; a5a2a1	$d_8e_7a_5a_4a_1$	6	2	neighbor
60	23	a8; a7a1; a4a4	$a_{13}a_7a_4a_1$	6	4	neighbor
60	23	a8; d5a3; a4a4	$e_8a_8d_5a_4$	6	3	neighbor
60	23	e6a2; a7a1; a4a4	$e_8a_7e_6a_4$	6	2	neighbor
60	23	e6a2; d5a3; a4a4	$a_8e_6d_5a_4a_2$	6	3	neighbor
60	22	e7a1; a4a4; e7a1, a8	$a_{11}e_7d_7$	6	2	
64	23	a7a1; a7a1; a7a1	$a_7^3a_1^4$	1	4	neighbor
64	23	a7a1; a7a1; d5a3	$A_7^2D_5^2$	3	4	deep hole neighbor
64	23	a7a1; d5a3; d5a3	E_8^3	3	4	deep hole neighbor
64	23	d5a3; d5a3; d5a3	D_8^3	1	4	deep hole neighbor
64	22	e7a1; a7a1; e7a1, d5a3	$d_{10}e_7d_7a_1$	6	2	
64	22	a7a1; a7a1; e8, a7a1	$a_{15}d_9a_1$	3	2	

Weight product	Intersection dimension	E_8^3 vertices not in intersection	Delaunay cells	Number of cells in this orbit	Magnitude of most remote vertex	Notes
72	23	e7a1; a5a2a1; a5a2a1	$e_7a_5^3a_1^3$	3	2	neighbor
72	23	d8; a5a2a1; a5a2a1	$D_{10}E_7^2$	3	3	deep hole neighbor
72	23	a8; a7a1; a5a2a1	$d_{10}a_8a_5a_2$	6	3	neighbor
72	23	a8; d5a3; a5a2a1	$a_{11}d_5a_5a_3a_1$	6	4	neighbor
72	23	e6a2; a7a1; a5a2a1	$a_7e_6^2a_5a_1$	6	2	neighbor
72	23	e6a2; d5a3; a5a2a1	$e_6d_5a_5^2a_2^2$	6	3	neighbor
72	22	a8; e8, a8; d8, a7a1	A_{24}	6	3	deep hole
72	21	d8; e8, d8; e6a2, a5a2a1	$d_{12}d_{10}a_2a_1$	6	2	
75	23	a8; a4a4; a4a4	$a_9a_4^2a_4^2$	3	5	neighbor
75	23	e6a2; a4a4; a4a4	E_8^3	3	5	deep hole neighbor
80	23	a7a1; a7a1; a4a4	$a_7^2d_5a_4a_1^2$	3	4	neighbor
80	23	a7a1; d5a3; a4a4	$a_9a_7d_5a_3a_1$	6	4	neighbor
80	23	d5a3; d5a3; a4a4	E_8^3	3	5	deep hole neighbor
80	22	e7a1; a7a1; e7a1, a4a4	$a_{13}d_{10}a_2$	6	2	
90	23	a8; a4a4; a5a2a1	$a_{14}a_4^2a_2a_1$	6	5	neighbor
90	23	e6a2; a4a4; a5a2a1	$e_6^2a_5a_4a_2^2$	6	3	neighbor
96	23	a7a1; a7a1; a5a2a1	$a_7^2a_5a_3a_1^2a_1$	3	4	neighbor
96	23	a7a1; d5a3; a5a2a1	$a_7^2d_5a_3a_2a_1$	6	4	neighbor
96	23	d5a3; d5a3; a5a2a1	$D_{10}E_7^2$	3	6	neighbor
100	23	a7a1; a4a4; a4a4	$a_9a_4^2a_4^2$	3	5	neighbor
100	23	d5a3; a4a4; a4a4	$d_5a_4^5$	3	5	neighbor
108	23	a8; a5a2a1; a5a2a1	E_8^3	3	6	deep hole neighbor
108	23	e6a2; a5a2a1; a5a2a1	E_6^4	3	6	deep hole neighbor
120	23	a7a1; a4a4; a5a2a1	$e_7a_7a_5a_4a_1a_1$	6	4	neighbor
120	23	d5a3; a4a4; a5a2a1	$a_9d_5a_4^2a_2a_1$	6	5	neighbor
125	23	a4a4; a4a4; a4a4	A_4^6	1	5	deep hole neighbor
144	23	a7a1; a5a2a1; a5a2a1	$a_7a_5^3a_1^3$	3	4	neighbor
144	23	d5a3; a5a2a1; a5a2a1	E_8^3	3	6	deep hole neighbor
150	23	a4a4; a4a4; a5a2a1	$a_5a_4^5$	3	5	neighbor
180	23	a4a4; a5a2a1; a5a2a1	E_8^3	3	6	deep hole neighbor
216	23	a5a2a1; a5a2a1; a5a2a1	E_6^4	1	6	deep hole neighbor

We summarize the proximity of the Delaunay cells described in table 7 to E_8^3 in table 8, where dim is the dimension of the intersection of the given cell with the central E_8^3, and mag is the magnitude of the cell vertex most remote from the central E_8^3. A check mark indicates the existence of cells with the given parameters, and a bold exclamation point indicates the enumeration is complete. An X indicates the non-existence of cells with the given parameters. An empty box indicates the enumeration has not been attempted above. The easiest open case to complete is that of cells that intersect the central E_8^3 in a 22-dimensional face, the magnitude of whose most remote vertex is 2.

Table 8. *Dimension and magnitude with respect to E_8^3 of cells in table 5.*

Dim↓ Mag→	0	1	2	3	4	5	6
24	!	X	X	X	X	X	X
23	X	!	!	!	!	!	!
22	X	X	✓	✓			
21	X	X	✓				
20	X	X	✓	✓			

Table 8 reveals a fact that is common to all deep holes, as well as a fact that is unique to E_8^3. With respect to every deep hole, "dim=24" is equivalent to "mag=0"; either condition states that the cell in question is the central deep hole itself. Consequently, any cell other than the central deep hole itself has dim<24 and mag>0. If the central deep hole is E_8^3, we may conclude further that "mag=1" implies "dim=23", the reason being that E_8^3 has only one star of magnitude 1; removal of this single vector from a cell satisfying mag=1 yields a 23-dimensional facet of E_8^3. The implication fails for other deep holes, however. For example, it may be seen in figure 2 that $A_{24} \subset D_{24} + 1$ and $D_{24} \subset A_{24} + 1$, but the intersection of A_{24} and D_{24} is the 22-dimensional simplex a_{23}.

An inspection of the neighbors of E_8^3 listed in table 7 reveals that there is an association between increasing weight products and increasing magnitude of the most remote vector. In fact, there is a strong correlation ($r \approx .8271$) between the cube root of the weight product and the magnitude of the most remote vector. This is depicted in figure 5 for the 165 orbits of neighbors of E_8^3. This phenomenon may be explained in part by considering the faces shared by E_8^3 and its neighbors, which are identified by removing one node from each of the three E_8 diagrams. Several of the low-magnitude stars of E_8^3 are connected to one node from each of the three E_8 diagrams, a node whose weight is equal to the magnitude of the star. Removal of those nodes allows the adjunction of that star to form the diagram for a neighboring shallow hole. Conversely, adjunction of a star of a given magnitude to one of the three E_8 diagrams in order to form a part of the diagram for a neighboring shallow hole is facilitated by removal of nodes of weight equal to the magnitude of the given star from the other two E_8 diagrams.

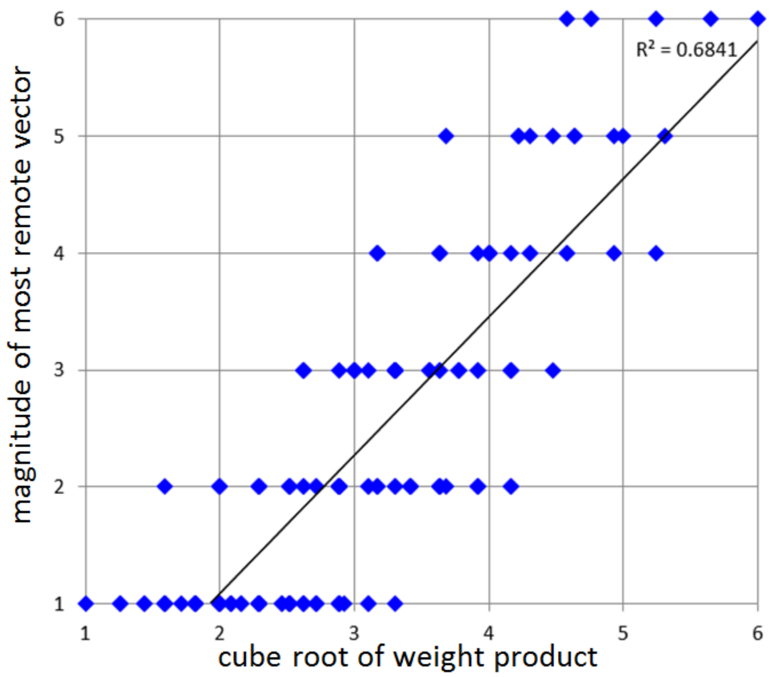

Figure 5. *Scatterplot of data about the 165 orbits of neighbors of E_8^3.*

7. Neighbors of Other Deep Holes

A complete atlas of the Leech lattice could be accomplished by constructing analogues of table 7 and figure 2 for every deep hole. That is, one could list every neighbor of every deep hole, and draw every deep hole (along with at least one of its glue vectors) from the point of view of every other deep hole. This project would be extremely tedious to carry out; but it is also unnecessary. In fact, the most detailed part of this project has been accomplished above. The reason why is a bit of a mystery, and is now discussed.

The longest lists of neighboring holes would be associated with the most diverse deep holes. But the most diverse deep holes tend to be very close to one another. Indeed, the three most diverse deep holes (E_8^3, $D_{10}E_7^2$, and $D_{16}E_8$) are full-fledged neighbors of one another; and other diverse deep holes (together with many of their own shallow hole neighbors) appear within E_8^3+n for small n. Thus, the work we put in to enumerate holes in the vicinity of E_8^3 provides the added benefit of displaying many members of the other long lists of holes in the vicinity of the other diverse deep holes. We should not be surprised that highly diverse deep holes share many neighbors, and are thus expected to be found in the vicinity of one another.

Consequently, to discover areas of the Leech lattice that are not in close proximity to E_8^3, we should go to the other end of the spectrum, and investigate the vicinity of the least diverse deep holes: holes with the smallest Coxeter numbers, the largest glue codes, and the largest automorphism groups. Even though those holes are the most multifaceted (they have the most faces), due to their large automorphism groups, they have very few orbits of neighbors, orbits which are relatively easy to enumerate. This enumeration is carried out in table 9 for a few deep holes.[xvi] We do not include the information regarding the dimension of intersection (always 23), the weight product for holes of the form $A_n^{24/n}$ (always 1 for such holes), or the name of the omitted nodes for holes of the form $A_n^{24/n}$ (always an within each component of $A_n^{24/n}$). As with table 7, we start with the deep hole diagram; systematically eliminate, in all possible ways, one node from each connected component of the diagram; and seek to complete this diminished diagram to the diagram of a hole, consistent with the graphical restrictions discussed above.[xvii] Perhaps an energetic reader will extend table 9 to cover more deep holes: in particular, $A_5^4D_4$ and A_6^4.

Table 9. *Neighbors of the most multifaceted deep holes.*

A_1^{24}		A_2^{12}		A_3^8		A_4^6	
Delaunay cells	**Number of cells in this orbit**	**Delaunay cells**	**Number of cells in this orbit**	**Delaunay cells**	**Number of cells in this orbit**	**Delaunay cells**	**Number of cells in this orbit**
$a_1^{24}a_1$	4096	$a_2^{12}a_1$	729	$a_3^8a_1$	256	$a_4^6a_1$	125
$a_2a_1^{23}$	98304	$a_3a_2^{11}$	17496	$a_4a_3^7$	4096	$a_5a_4^5$	1500
$a_3a_1^{22}$	1130496	$a_5a_2^{10}$	192456	$d_4a_3^7$	2048	$d_5a_4^5$	1500
$d_4a_1^{21}$	8290304	E_6^4	320760	$a_7a_3^6$	28672	$a_9a_4^2a_4^2$	7500
D_4^6	7254016			$d_7a_3^6$	28672	E_8^3	5000
				D_6^4	1792		

D_4^6			
Weight product	**Vertices not in intersection**	**Delaunay cells**	**Number of cells in this orbit**
1	d4, d4, d4, d4, d4, d4	$d_4^6a_1$	64
1	d4, d4, d4, d4, d4, d4	$d_5d_4^5$	1152
1	d4, d4, d4, d4, d4, d4	D_8^3	2880
2	d4, d4, d4, d4, d4, a1^4	$d_4^5a_2a_1^3$	384
2	d4, d4, d4, d4, d4, a1^4	$d_6d_4^4a_1^3$	5760
4	d4, d4, d4, d4, a1^4, a1^4	$d_4^4a_3a_1^6$	960
4	d4, d4, d4, d4, a1^4, a1^4	D_8^3	2880

D_4^6			
Weight product	**Vertices not in intersection**	**Delaunay cells**	**Number of cells in this orbit**
8	d4, d4, d4, a1^4, a1^4, a1^4	$d_4^4a_1^9$	320
8	d4, d4, d4, a1^4, a1^4, a1^4	$d_4^4a_3a_1^6$	960
16	d4, d4, a1^4, a1^4, a1^4, a1^4	D_4^6	240
32	d4, a1^4, a1^4, a1^4, a1^4, a1^4	$d_4a_1^{21}$	24
64	a1^4, a1^4, a1^4, a1^4, a1^4, a1^4	A_1^{24}	1

Imagine a journey through the Delaunay tessellation of R^{24} created by the Leech lattice, starting at a random point (but not a lattice point or a hole), and proceeding slowly in a generic direction (all ratios of coordinates of the direction vector should be irrational, as computed in the standard A_1^{24} coordinate system). We may expect to visit all Delaunay cells eventually. We might also anticipate a roughly equal distribution of time spent in interesting neighborhoods, with a large diversity of cells, and in uninteresting neighborhoods, with a small diversity of cells - but this anticipated itinerary would be mistaken. As we have seen, most of the journey will be spent in diverse neighborhoods; moreover, these tend to cluster together. The journey will be interrupted only rarely by passing through isolated non-diverse neighborhoods.

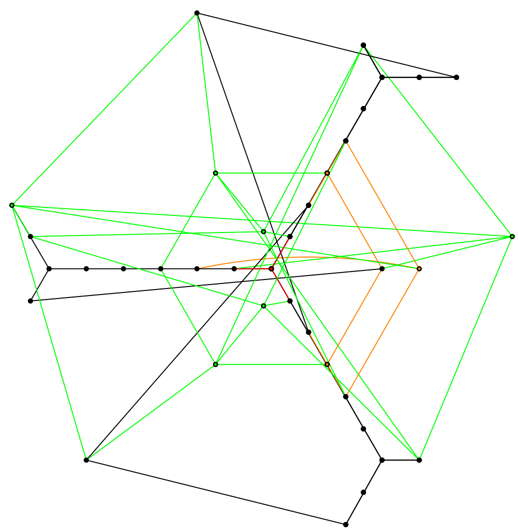

Figure 6. *An additional copy of E_8^3+3.*

8. Concepts, Connections, Conjectures, and Some Proofs

8.1. A Combinatorial View of the Leech Lattice

Conway [10] conjectured that there may be a purely combinatorial, graphical description of the Leech lattice based on the known restrictions on deep hole diagrams described above, and on the “starry” coordinate system described above. The conjecture depends on Borcherds’s identification of the 23 deep holes in the Leech lattice with the 23 Niemeier lattices of minimal norm 2 in [3], and Venkov’s classification in [24], chapter 18, of the self-dual codes corresponding to those 23 root systems. The root systems correspond to the hole vertices, while the self-dual codes correspond to the glue vectors. That is, for each of the 23 deep holes X, the graph $X+1$ (including hole vertices and glue vectors) is known and unique. The idea would be to begin at a deep hole, say of type X, together with its glue vectors, locating new deep hole diagrams in the enlarged diagram $X+1$. One then affixes glue vectors to the new deep holes, and then repeats the construction from the new deep holes, and so on, eventually filling all of R^{24} with the Leech lattice.

It may be possible to achieve such a goal by starting at the apparently ubiquitous deep hole E_8^3. As we saw above in Figure 1, the graph E_8^3+3 includes (copies of) 12 distinct deep holes in their entirety together with some of their attendant glue vectors, as well as partial diagrams for 8 more deep holes; the remaining 3 deep holes are neighbors of some of the 20 deep holes so far mentioned; and among the numerous neighbors of E_8^3 are many new copies of E_8^3 itself.

For the reader’s convenience, one such new copy of E_8^3 is displayed in figure 6; it has weight product 18 with respect to the original E_8^3. Comparing the new and original copies of E_8^3, we see that each E_8^3 is included in the other E_8^3+3, each E_8^3+1 is included in the other E_8^3+3, each E_8^3+2 is included in the other E_8^3+4, and each E_8^3+3 is included in the other E_8^3+4. There is an orbit of three such new copies of E_8^3 under the automorphism group of the original E_8^3. We can repeat the construction of this orbit, but this time starting at one of the new copies of E_8^3, such as the one pictured in figure 6. One of the three second-generation copies of E_8^3 so created is the original E_8^3. The other two second-generation copies appear to be new. If so, then by repeating the construction, we get an infinite collection of E_8^3 holes, each of which neighbors three others in the collection; presumably their centers lie in a 2-dimensional plane, and form the vertices of the regular hexagonal tessellation $\{6,3\}$.

Conway's conjecture may be related to another conjecture about lattices that has never been proven or disproven, as far as the author knows, namely, that every shallow hole Delaunay cell in every lattice shares an $(n-1)$-dimensional face with a deep hole Delaunay cell, where n is the dimension of the lattice. We have no evidence to suggest that this conjecture is true in general, but it appears to be true for the Leech lattice - and even more. A quick perusal of the list of shallow holes in [24], chapter 25, appears to imply that every shallow hole in the Leech lattice is a full-fledged close neighbor of some deep hole, although this has never been proven either.

8.2. The Genus, Theta Series, and Canonical Notation for a Lattice

Every finite-dimensional integral lattice can be described by a finite amount of information: namely, its Gram matrix (see [24], chapter 1). Thus an n-dimensional integral lattice may be described by an element of $Z^{n(n+1)/2}$. Seeking a more compact notation, we consider two invariants of the lattice: namely, its genus (see [24], chapter 15) and its theta series (see [24], chapter 2). Lattices in the same genus need not have the same theta series; for example, consider the 24 Niemeier lattices, only one of which (the Leech lattice) lacks elements of norm 2. Lattices with the same theta series need not be in the same genus; an example is given in the preface to the third edition of [24]. If there were a finite notation for both the genus and the theta series of a lattice, one might hope for a short symbolic identification of any integral lattice by conjoining the two notations. Unfortunately, lattices in the same genus (congeneric) and with the same theta series (isospectral) need not be isomorphic; consider the examples of E_8^2 and D_{16}^+, or D_{12} and E_8D_4. Among the 24 Niemeier lattices, which are the 24 members of one genus, there are five isospectral pairs: namely, those pairs of lattices sharing a Coxeter number.

Conway and Sloane provide a finite notation for the genus. In contrast, the theta series is infinite, but may perhaps be determined by a finite initial segment, if the following conjecture is true. Call μ' the *generating norm* of a lattice Λ if Λ can be generated by all its elements of norm no greater than μ', and μ' is the smallest number with this property. $\mu' \geq \mu$, where μ is the minimal norm of the lattice. Merely knowing the theta series of Λ as far as elements of norm μ' does not determine the entire theta series or even the dimension of Λ. For example, the theta series of A_2 and A_1^3 (two lattices with generating norm 2) both begin: $1+6q^2$. However, the theta series of these lattices are seen to differ once we include terms representing elements of twice the minimal norm. Now, the initial segments of these theta series are $1+6q^2$ for A_2, but $1+6q^2+12q^4$ for A_1^3. Thus we conjecture that a theta series is determined by its finite initial segment including terms representing all elements up to twice the generating norm. This conjecture is plausible because, for example, if a lattice is generated by its minimal vectors, sums of minimal vectors will have norm no more than twice the minimal norm, unless the lattice is $\mathbb{Z}$ or A_2.[xviii]

One may abbreviate the theta series (or an initial segment thereof) still further by eliminating the first term 1, common to all theta series, and eliminating the plus signs and the variable. Assuming the conjecture above is true, table 10 provides the following canonical notations for some well-known lattices discussed repeatedly below.

Table 10. *Canonical notation for lattices.*

Lattice (usual name)	Canonical notation	Extended canonical notation
$\mathbb{Z}$	$\mathrm{I}_1(1){:}2^1$	$\mathrm{I}_1(1){:}2^1{:}[2]$
A_2	$\mathrm{II}_2(3^{-1}){:}6^2$	$\mathrm{II}_2(3^{-1}){:}6^2{:}[6{:}2]$
$\mathbb{Z}^2$	$\mathrm{I}_2(1){:}4^1 4^2$	$\mathrm{I}_2(1){:}4^1 4^2{:}[4{:}2]$
D_4	$\mathrm{II}_4(2_{\mathrm{II}}^{-2}){:}24^2 24^4$	$\mathrm{II}_4(2_{\mathrm{II}}^{-2}){:}24^2 24^4{:}[2{:}(\mathrm{Alt}_4)^2{:}2^2]$
E_8	$\mathrm{II}_8(1){:}240^2 2160^4$	$\mathrm{II}_8(1){:}240^2 2160^4{:}[2{:}\mathrm{O}_8^+(2){:}2]$
Λ_{24}, the Leech lattice	$\mathrm{II}_{24}(1){:}196560^4 16773120^6 398034000^8$	$\mathrm{II}_{24}(1){:}196560^4 16773120^6 398034000^8{:}[\mathrm{Co}_0]$

It is very unlikely that this proposed notation will replace the commonly known nomenclature any time in the foreseeable future. Nevertheless, the prospect arises of a program to describe all integral lattices. One step in this program would be to determine what strings of symbols constitute permissible notations for lattices. Another step would be to determine a bound on the number of lattices that may share a given permissible notation. The non-isomorphic lattices described above that share the same genus and the same theta series may nevertheless be distinguished by their automorphism groups. If so, an extended canonical notation should describe at least the order of the lattice's automorphism group, if not the group itself. Such notation is provided in the last column of table 7. The group notation is very much non-canonical; for example, the groups for the lattices D_4 and E_8 could have been rendered as $W(F_4)$ and $W(E_8)$.

8.3. Modest and Robust Lattices

Low-dimensional lattices can rapidly accumulate automorphism groups containing elements of large order. For example, the 6-dimensional lattice A_4A_2 is stabilized by an automorphism of order 30; the 12-dimensional lattice $A_6A_4A_2$ is stabilized by an automorphism of order 210; the 22-dimensional lattice $A_{10}A_6A_4A_2$ is stabilized by an automorphism of 2310, and so on. Even an irreducible lattice like the 20-dimensional A_{20} is stabilized by an automorphism of order 630. At the other extreme, of course, there are many lattices with trivial automorphism groups of order 2. It is remarkable that some important lattices, like E_8, the Leech lattice, and others, have irreducible automorphism groups and high degrees of symmetry as described elsewhere in this section, but with limits on the orders of individual automorphisms.

Before we elaborate, we define a canonical lattice L_m with irreducible automorphism group associated with every even natural number m. L_m has exactly m minimal vectors. The dimension of L_m is $\varphi(m)$, where φ is Euler's totient function, the number of natural numbers not exceeding m which are relatively prime to m. Let the prime factorization of m be $m=\prod_{i=1}^{k} {p_i}^{e_i}$, where the p_i are distinct primes, $p_1=2$, and the e_i are natural numbers. Then L_m is defined to be the following lattice:

$$L_m \cong \otimes_{i=1}^{k} \left(A_{p_i-1}^{*}\right)^{\left({p_i}^{(e_i-1)}\right)} \cong \otimes_{i=1}^{k} \left(\left(A_{p_i-1}\right)^{\left({p_i}^{(e_i-1)}\right)}\right)^{*} \cong \left(\otimes_{i=1}^{k} \left(A_{p_i-1}\right)^{\left({p_i}^{(e_i-1)}\right)}\right)^{*}$$

L_m has an automorphism of order m, which is the product of automorphisms of order ${p_i}^{e_i}$ of the respective factors in the tensor product. Thus a cyclic group of order m, where m is even, has a crystallographic representation in $\varphi(m)$ dimensions (that is, it is a subgroup of $GL_{\varphi(m)}(\mathbb{Z})$).[xix] Table 11 lists low-dimensional examples of the lattices L_m, described up to similarity. We simplify the results by recalling that A_1^* is similar to $\mathbb{Z}$, and A_2^* is similar to A_2.

Table 11. *Low-dimensional cases of the lattices L_m.*

m	φ(m) = dim L_m	Similarity class of L_m
2	1	$\mathbb{Z}$
4	2	$\mathbb{Z}^2$
6		A_2
8	4	$\mathbb{Z}^4$
10		A_4^*
12		A_2^2
14	6	A_6^*
18		A_2^3
16	8	$\mathbb{Z}^8$
20		$(A_4^*)^2$
24		A_2^4
30		$A_2 \otimes A_4^*$
22	10	A_{10}^*

An n-dimensional *modest lattice* Λ is well-behaved in the following sense. Let Λ have an automorphism of order m; then in a modest lattice, we must have $\varphi(m) \le n$. An interesting open question is whether this property is equivalent to the statement that Λ is commensurable with L_m, where lattices A and B are *commensurable* (which we shall write symbolically as $A \approx B$) provided $A \cap B$ has finite index in whichever of A and B has smaller dimension, or has finite index in both A and B if they have equal dimension. A_n and A_n^* for $n \le 8$ but $n \ne 7$, D_n and D_n^* for $n \le 9$, E_6, E_6^*, E_8 and the Leech lattice are all modest lattices, among other lattices that are mentioned in this section; but A_7, A_7^*, E_7, and E_7^* have automorphisms of order 15, despite the fact that $\varphi(15)=8$. E_8 is known to be commensurable with most L_m for $\varphi(m) \le 8$, with the only unknown case being $m=30$. In contrast, A_n and A_n^* for $n \ge 9$, and D_n and D_n^* for $n \ge 10$ are not modest. For example, the automorphism group of A_9 (and its dual) contains an element of order 21, but $\varphi(21)=12$; the automorphism group of D_{12} (and its dual) contains an element of order 35, but $\varphi(35)=24$; the automorphism group of D_{21} (and its dual) contains an element of order 630, but $\varphi(630)=144$, and so on.

We define Λ to be a *robust lattice* if it has an automorphism of order m whenever $\varphi(m) \le \dim(\Lambda)/2$. E_8 and the Leech lattice are modest, robust lattices with irreducible automorphism groups. It would be useful to enumerate all modest, robust lattices with irreducible automorphism groups.

Table 12 displays all natural numbers m such that $\varphi(m) \le 24$; the orders of elements of $\mathrm{Aut}(\Lambda_{24})$ are displayed in bold. Despite the Leech lattice's modesty, the order of its automorphism group is divisible by all primes less than 29 with the exceptions of 17 and 19. Even here, however, we note that by the holy constructions of the Leech lattice described in [24], chapter 24, the Leech lattice is commensurable with all of the remaining Niemeier lattices, including those of types A_{24} and D_{24}, whose automorphism groups contain elements of order 17 and 19. Thus there are sublattices of the Leech lattice with automorphisms of order equal to the missing primes. We conjecture that the Leech lattice is commensurable with all L_m for $\varphi(m) \leq 24$.

Table 12. Natural numbers with small totient values.

n	m such that $\varphi(m) = n$
1	1,2
2	3,4,6
4	5,8,10,12
6	7,9,14,18
8	15,16,20,24,30
10	11,22
12	13,21,26,28,36,42
16	17,32,34,40,48,60
18	19,27,38,54
20	25,33,44,50,66
22	23,46
24	35,39,45,52,56,70,72,78,84,90

The conjecture is provable in many cases.

The Leech lattice is commensurable with L_m for $\varphi(m) \leq 24$ and *m* not divisible by two distinct odd primes. In this case, L_m is similar to an integer lattice (when *m* is a power of 2) or a power of A_{p-1}^* (when *m* is divisible by exactly one odd prime, *p*). All such lattices are commensurable with some Niemeyer lattice, which in turn is commensurable with the Leech lattice, by the holy construction outlined in [24], chapter 24.

The Leech lattice is commensurable with L_m for $\varphi(m) < 22$. This depends on a remarkably strong theorem from [15] about embeddings of integral lattices into other integral lattices. A powerful corollary to this theorem asserts that if *A* and *B* are any integral lattices such that $\dim(B) \geq \dim(A) + 3$, then *A* is similar to a sublattice of *B*.[xx] Therefore, *A* is commensurable with *B*, and this establishes the present claim.

Consequently the conjecture is open only for $m = 70, 78, 84, 90$.

The commensurability of the Leech lattice with other lattices is addressed in part in [19].

We define the *order spectrum* of a group to be the set of orders of the group's elements. When every element of the group has finite order, this set of natural numbers is closed downward under divisibility. As such, it is a subset of the natural numbers with multiplication, conceived as the free abelian monoid on countably infinitely many generators (the prime numbers). We visualize the order spectrum of a group, when it is finite, through projection. We illustrate the order spectrum of $\mathrm{Aut}(E_8)$ in figure 7. In these diagrams, the black node in the lower left represents 1. Movement up and to the right along any edge represents multiplication by a prime number: 2 for dark red edges, 3 for medium blue edges, 5 for light green edges, 7 for bright purple edges, and so on, with the slope of the edges increasing with the size of the prime number. The colors of the edges and of the nodes are taken from [20], the Periodic Table of Numbers.[xxi]

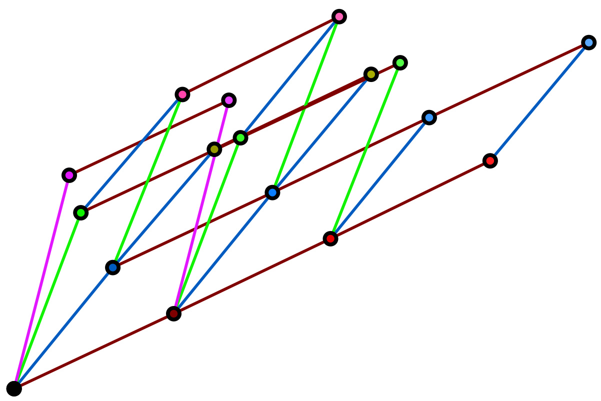

Figure 7. Graph of the (cyclic) order spectrum of $Aut(E_8)$.

In a similar fashion, we can define the *abelian order spectrum* and the *nilpotent order spectrum* of a group to be the set of orders of all abelian (respectively, nilpotent) subgroups; our original order spectrum might be described as the cyclic order spectrum. These two new sets are also closed downward under divisibility, but they will not be illustrated.

8.4. Coxeter-celled Lattices

We say that a lattice is *Coxeter-celled* if all of its Delaunay cells are described by unions of Coxeter-Dynkin diagrams of finite or extended type. Define the *covering ratio* of a lattice to be R/ρ, where R is the covering radius and ρ is the packing radius ([10]). This quantity is also described as the packing-covering constant, and is investigated, in [25] and [26]. A Coxeter-celled lattice necessarily has covering ratio no more than $\sqrt{2}$; see [24], chapter 23. Table 13 enumerates the known Coxeter-celled lattices, which all happen to be sections, as well as projections, of the Leech lattice. We conjecture that this list is complete, but have not been able to prove it. It appears that the Leech lattice may well be the largest-dimensional lattice with covering ratio $\sqrt{2}$ or less; but proving this is difficult.

Table 13. *Known Coxeter-celled lattices.*

Dimension	Name (up to similarity)	Minimal norm	Delaunay cells	Covering ratio
1	$\mathbb{Z}$	4	a_1^2	1
1	$\mathbb{Z}$	6	a_2	1
1	$\mathbb{Z}$	8	A_1	1
2	$\mathbb{Z}^2$	4	A_1^2	$\sqrt{2}$
2	A_2	4	a_1^3	$\sqrt{4/3}$
2		4	$a_2 a_1$	?
2		4	a_3	?
2	A_2	6	A_2	$\sqrt{4/3}$
3		4	A_3	$\sqrt{2}$
3	$A_3 \cong D_3$	4	$A_1^3,\ a_1^4$	$\sqrt{2}$
4	A_4^*	4	A_4	$\sqrt{2}$
4	$A_2 \otimes A_2$	4	$A_2^2,\ a_2^2 a_1$	$\sqrt{2}$
4	D_4	4	A_1^4	$\sqrt{2}$
6	E_6^*	4	A_2^3	$\sqrt{2}$
8	E_8	4	$A_1^8,\ a_1^9$	$\sqrt{2}$
24	Λ_{24}, the Leech lattice	4	23 deep, 284 shallow	$\sqrt{2}$

8.5. Pretty Lattices

The most interesting lattices tend to have irreducible automorphism groups, or have automorphism groups that are locally multiply transitive on minimal vectors, or both. We say that an n-dimensional lattice Λ is *1-pretty* provided its automorphism group acts irreducibly in R^n and transitively on minimal vectors; this property is shared by all the irreducible root lattices and their duals, for example. Λ is *2-pretty* provided it is 1-pretty, and given any minimal vector v, the stabilizer of v (and the origin) acts irreducibly in R^{n-1} and acts transitively on the non-empty set of minimal vectors of Λ that are at the minimal distance from v; thus Aut(Λ) acts transitively on minimal regular triangles (and the irreducibility conditions guarantee that there are many such triangles). Λ is *3-pretty* provided it is 2-pretty, and given a minimal regular triangle, its pointwise stabilizer acts irreducibly in R^{n-2} as well as transitively on the non-empty set of minimal vectors at the minimal distance from all vertices of the given triangle; thus Aut(Λ) acts transitively on minimal regular tetrahedra (of which there must be many); and so on. Table 14 enumerates the known 2-pretty lattices, which all happen to be sections, as well as projections, of the Leech lattice. We conjecture that this list is complete, but have not been able to prove it.[xxii]

Table 14. *Known 2-pretty lattices.*

Dimension	Name (up to similarity)	Degree of prettiness
2	A_2	2
4	A_2^2	2
4	$A_2 \otimes A_2$	2
4	D_4	3
6	E_6^*	2
7	E_7	3
8	E_8	5
23	Λ_{23}	2
24	Λ_{24}, the Leech lattice	4

The known 4-pretty lattices, E_8 and Λ_{24}, have interesting series of minimal regular simplex stabilizers, which are enumerated in Table 15. Here, we let p equal the number of minimal vectors at mutually minimal distances that are being stabilized pointwise, in addition to the origin. These $p+1$ points form a minimal p-dimensional regular simplex α_p (in Coxeter's notation). Its pointwise stabilizer acts in R^{n-p}, where n = dim(Λ); and irreducibly so, when Λ is $(p+1)$-pretty. $W(X)$ is the Weyl reflection group of type X; see [11].

Table 15. *Stabilizers of minimal regular simplexes in* E_8 *and* Λ_{24}.

p	E_8 Stabilizer of minimal α_p	E_8 Number of minimal vectors whose adjunction yields minimal α_{p+1}	Λ_{24} Stabilizer of minimal α_p	Λ_{24} Number of minimal vectors whose adjunction yields minimal α_{p+1}
0	$W(E_8)$	240	$Co_0 \cong\cdot 0 \cong \mathrm{Aut}(\Lambda_{24})$	196560
1	$W(E_7)$	56	$Co_2 \cong\cdot 2 \subseteq \mathrm{Aut}(\Lambda_{23}^*)$	4600
2	$W(E_6)$	27	$U_6(2) \subseteq \mathrm{Aut}(\Lambda_{22}^*)$	891
3	$W(D_5)$	16	$2^9: M_{21} \subseteq \mathrm{Aut}(\Lambda_{21}^*)$	336
4	$W(A_4)$	10	$2^5: M_{20}$	2 orbits of sizes 10 and 160
5	$W(A_2A_1)$ (reducible)	6		
6		2 orbits of sizes 1 and 2		

8.6. The Reach of a Lattice

Another way to measure high degrees of symmetry in lattices is to consider the transitivity of the automorphism group of the lattice upon successively larger shells of the lattice - sets of lattice vectors at a given distance from the origin. Let Λ be an integral lattice with minimal norm μ. (We only consider integral lattices, because otherwise the following definition would not make sense.) The automorphism group of Λ acts on the various shells of Λ, and we inquire how many of these shells have just one orbit under Aut(Λ). Specifically, let k be the smallest rational number such that Aut(Λ) fails to act transitively on the (non-empty) shell of lattice vectors whose norm is $k\mu$; if no such rational number exists, then $k=\infty$. We refer to k as the *reach* of Λ. If Aut(Λ) fails to act transitively on even its minimal vectors, then $k=1$. The larger k is among lattices of a given dimension, the more symmetric Λ is.

In table 16, we enumerate a set of nine lattices that have an unusually large reach for their dimensions, and we conjecture that these lattices are somehow optimal, in the following sense. Every integral lattice in more than 1 dimension has finite reach. (This much is certainly true; it follows from the finitude of Aut(Λ), combined with the unbounded cardinalities of the shells of Λ.) Any integral lattice in more than 1 dimension whose reach is more than 9 must be isomorphic to A_2 or $\mathbb{Z}^2$. Any integral lattice in more than 2 dimensions with reach greater than 4 must be isomorphic to $\mathbb{Z}^3$, $A_3 \cong D_3$, $A_3^* \cong D_3^*$, or D_4.[xxiii] Any integral lattice in more than 4 dimensions with reach greater than 3 must be isomorphic to E_8. Any integral lattice in more than 8 dimensions with reach greater than 2 must be isomorphic to the Leech lattice. Again, these statements are conjectures.

Table 16. *Lattices with many single-orbit shells under Aut(Λ).*

Dimension	Name (up to similarity)	Reach
1	$\mathbb{Z}$	∞
2	A_2	49
2	$\mathbb{Z}^2$	25
3	$\mathbb{Z}^3$	9
3	$A_3 \cong D_3$	9
3	$A_3^* \cong D_3^*$	9
4	D_4	9
8	E_8	4
24	Λ_{24}, the Leech lattice	3

It would be useful to enumerate all lattices with reach greater than or equal to 3.

8.7. Prompt Lattices

We call attention to a small class of lattices that are similar to their duals and arise as the smallest self-dual lattices over Euclidean rings of algebraic integers, in the lowest dimension in which such a self-dual lattice is possible. We start with the nested series of rings of the form $\mathbb{Z}[2Alt_n]$, with n = 2, 3, 4, or 5. This notation appears in [29]. These rings are otherwise known as the real rational integers $\mathbb{Z}$, the Eisenstein complex integers E, the Hurwitz quaternionic integers H, and the dense quaternionic ring of icosians I, orders of ranks 1, 2, 4, and 8 respectively. [24], chapter 7, supplies several upper bounds for the minimal norm μ of self-dual lattices Λ over various rings J, which imply that in general, $\mu \leq [n/d] + 1$, where n is the dimension of Λ and d is the *critical dimension*: the smallest dimension in which a self-dual lattice with minimal norm 2 exists over J. When $\mu = [n/d] + 1$, we say Λ is *extremal* self-dual over J.

We say that Λ is *prompt* over a Euclidean ring of integers J if it is self-dual over J and arises in the smallest possible dimension; that is, $n = \max(1, (\mu - 1)d)$. As such, the lattice is extremal self-dual over J. The real versions of the known prompt lattices are interesting lattices, with high degrees of symmetry and packing efficiency. The known prompt lattices are listed in table 17. X means that a prompt lattice with the given parameters does not exist, while ? means that the lattice's existence is an open question. Note that the real versions of self-dual E-lattices are 3-modular; the real versions of self-dual H-lattices are 2-modular; and the real versions of self-dual I-lattices are even self-dual. Modularity is introduced briefly in the preface to the third edition of [24]. Tables of modular lattices are provided at the invaluable online Catalogue of Lattices [5].

Table 17. *Known prompt lattices.*

Ring J	$\mu = 1$		$\mu = 2$		$\mu = 3$		$\mu = 4$	
	Dimension over J	**Real lattice**	**Dimension over J**	**Real lattice**	**Dimension over J**	**Real lattice**	**Dimension over J**	**Real lattice**
$\mathbb{Z}$	1	$\mathbb{Z}$	8	E_8	16	X	24	Λ_{24}
E	1	A_2	6	K_{12}	12	X	18	?
H	1	D_4	4	Λ_{16}	8	X	12	?
I	1	E_8	3	Λ_{24}	6	?	9	?

The existence of a prompt 9-dimensional icosian lattice would be particularly significant. The real version of such a lattice would be an extremal Type II (even self-dual) lattice in 72 dimensions; see [24], chapter 7. An extremal type II lattice in R^{72} was found by Nebe; see [18]. Such a lattice would be a good candidate to prolong the sequence of laminated lattices (see [24], chapter 6) to 72 dimensions. We discuss the implications of such a lattice in the language of [7]: namely, integral laminated lattices. The notation $\Lambda_n^J[\mu]$ signifies an n-dimensional integral laminated lattice with minimal norm μ over the Euclidean ring of integers J; the latter is omitted when J = $\mathbb{Z}$. In our discussion, we laminate over $\mathbb{Z}$ unless otherwise specified. The sequences of integral laminated lattices discussed below are nested, up to similarity. That is, $\Lambda_n[4] \cong \sqrt{2}\Lambda_n[2]$ for $n \leq 8$, and $\Lambda_n[8] \cong \sqrt{2}\Lambda_n[4]$ for $n \leq 24$.

When we laminate lattices at minimal norm 2, they remain integral up through dimension 8, and $\Lambda_8[2] \cong E_8$, which is unimodular at minimal norm 2; further, the determinants of $\Lambda_n[2]$ and $\Lambda_{8-n}[2]$ are equal for n between 0 and 8 inclusive. When we laminate lattices at minimal norm 4, they remain integral up through dimension 24, and $\Lambda_{24}[4]$, the Leech lattice, is unimodular at minimal norm 4; further, the determinants of $\Lambda_n[4]$ and $\Lambda_{24-n}[4]$ are equal for n between 0 and 24 inclusive. Laminated lattices have been constructed so far only through dimension 48, but at minimal norm 8, they are integral; most fascinating is that the determinants of $\Lambda_n[8]$ and $\Lambda_{72-n}[8]$ are equal for n between 24 and 48 inclusive, suggesting that they are complementary sections of a 72-dimensional even, self-dual lattice in 72 dimensions. It appears that the Leech lattice is a section of Nebe's lattice, making plausible (although not yet certain) the identification between her lattice and an instance of $\Lambda_{72}[8]$. Presuming this identification exists, it would be interesting to know if there are any significant consequences of the analogy:

$$\Lambda_{24}[4]/(\Lambda_{24}[4] \cap (\Lambda_8[2])^3) \cong 2^4,$$

while

$$\Lambda_{72}[8]/(\Lambda_{72}[8] \cap (\Lambda_{24}[4])^3) \cong 2^{12}.$$

The elegance of these relations is obscured by the intricate notation, so we restate as follows. Let A, B, and C, respectively, signify the lowest dimensional even self-dual lattices at minimal norms 2, 4, and 8, respectively, with the caveat that C may not be unique, so that A is E_8, B is the Leech lattice, and C is (for example) Nebe's lattice. Then there exist embeddings of A^3 into the space of B and of B^3 into the space of C such that:

$$B/(B \cap A^3) \cong 2^4, \text{ while } C/(C \cap B^3) \cong 2^{12}.$$

8.8. The Shape Parameter of a Lattice

There is a curious real-valued function of lattices whose range appears to include both an interval and isolated points. We define the *shape parameter* of a lattice to be d_2/R, where d_2 is the distance from the origin to the closest lattice vector that is not a minimal vector (that is, d_2^2 is the second-smallest norm of non-zero lattice elements), and R is the covering radius of the lattice. Let ρ be the packing radius of the lattice, and μ its minimal norm, so that $\sqrt{\mu} = d_1 = 2\rho$. The shape parameter is thus equal to $(d_2/\rho)/(R/\rho)$, which in turn equals $2(d_2/d_1)/(R/\rho)$. For five lattices discussed in greater detail below ($\mathbb{Z}$, A_2, $\mathbb{Z}^2$, D_4, and E_8, for which the shape parameter equals 4, 3, 2, 2, and 2 respectively), the set of lattice vectors in the second shell coincides with the set of deep holes near the origin, multiplied by the shape parameter.

We call a lattice *busy* if its minimal vectors generate a lattice with the same dimension as the whole lattice. This happens, for example, if the lattice is generated by its minimal vectors. Table 18 enumerates busy lattices known to have shape parameter 2 or larger.

Table 18. *Busy lattices with large shape parameter.*

Dimension	Lattice	Shape parameter
1	$\mathbb{Z}$	4
2	A_2	3
2	$\mathbb{Z}^2$	2
3	$A_3 \cong D_3$	2
4	D_4	2
8	E_8	2

We can partially characterize the range of the shape parameter.

Theorem. The shape parameter of $\mathbb{Z}$ is 4; of A_2 is 3; and of every other busy lattice, is no more than $2\sqrt{1+1/n}$, where n is the dimension of the lattice.

Proof. Note that for any lattice Λ, $d_2/d_1 \le 2$, while $R/\rho \ge 1$; thus the shape parameter is always a positive number no more than 4. The shape parameter can only equal 4 when $d_2/d_1 = 2$ and $R/\rho = 1$; that is, $\Lambda \sim \mathbb{Z}$.

Below, we go into greater detail to establish a Rogers-type lower bound on the covering ratio. For the moment, suffice it to say that for an n-dimensional lattice, $R/\rho \ge \sqrt{2n/(n+1)}$. We note interesting features of the ratios that comprise the shape parameter: R/ρ and d_2/d_1. The former, the covering ratio, is a continuous function of a lattice basis, because R is the circumradius and ρ is the inradius of the Voronoi cell; while the latter ratio may be discontinuous as a function of the basis.

If the shape parameter is less than 4, then $R/\rho > 1$; consequently $n > 1$, so $R/\rho \ge \sqrt{4/3}$. If $R/\rho = \sqrt{4/3}$, then $n = 2$, and $\Lambda \sim A_2$, with $d_2/d_1 = \sqrt{3}$, and the shape parameter is 3.

It remains to be shown that if $R/\rho > \sqrt{4/3}$, then the shape parameter is no more than $2\sqrt{1+1/n}$. Note that once $n > 1$, assuming that Λ is busy and not similar to A_2, then $d_2/d_1 \le \sqrt{2}$, so the shape parameter is no more than $(2\sqrt{2})/\sqrt{2n/(n+1)} = 2\sqrt{1+1/n}$.

It would be useful to enumerate all busy lattices with shape parameter at least $\sqrt{3}$, the shape parameter of the Leech lattice, or at least with shape parameter at least 2, the limit of our bound as n increases. We conjecture that table 16 completely enumerates the busy lattices with shape parameter at least 2.

8.9. Tight Lattices

There is a select club of six lattices - $\mathbb{Z}$, A_2, $\mathbb{Z}^2$, D_4, E_8, and Λ_{24} - that combine unusually efficient packing (as measured by their small covering ratios and large contact numbers) with an unusually high degree of symmetry (as measured by their prettiness). Of the six lattices, only $\mathbb{Z}^2$ fails to be the densest lattice packing and to have the largest contact number in its dimension. The first five of these six lattices inherit their strong properties by virtue of being the lattices underlying nested discrete Euclidean sub-rings of the real numbers, complex numbers (twice), quaternions, and octonions, and the fact that each (other than $\mathbb{Z}^2$) is the densest 2-dimensional lattice over a ring of integers in half the number of dimensions.[xxiv] There is, as yet, however, no known algebraic structure on R^{24} that explains the Leech lattice; perhaps some exotic vector-product algebra over the octonions remains to be discovered.[xxv] The ring structure does imply an important lattice property which we call tightness, and have only observed in these six lattices; tightness, in turn, explains the small covering ratios, as well as the large contact numbers.

Let Λ be an n-dimensional lattice. Let $f: \Lambda \to \Lambda$ be simultaneously an endomorphism and a similarity that multiplies all norms (squared distances from the origin) by the natural number $t > 1$. Such functions can be defined trivially for any lattice Λ by multiplying its elements by an integer whose absolute value is greater than 1. Typically, Λ is a lattice over some Euclidean ring of algebraic integers, and f is defined as multiplication by an element x of that ring whose norm is t. Construction E, discussed in [24], chapter 8, makes use of such functions to build sequences of quite dense lattices in large dimensions. Conway and Sloane describe f as a type of a screw map, which is a composition of a translation and a rotation; but it would be more accurate to describe it as a composition of a dilation and a rotation. In the examples given below, we will use the following numbers of norms 9, 7, 5, 4, 3, and 2, namely: 3; $2-\omega$; $2+i$; 2; $1-\omega$; and $1+i$; where ω is a primitive cube root of 1, and i is a square root of -1.

We say that Λ is *t-tight* if all its vectors are congruent to the zero vector or to a minimal vector, modulo $f(\Lambda)$, and if Λ has the maximal possible contact number subject to the previous condition. This maximal possible contact number is, in general, $\tau = c(t,n)(t^{n/2}-1)$, where $c(t,n)$ represents the maximal number of minimal vectors in an n-dimensional lattice that may be at mutual squared distance t, assuming that minimal vectors are one unit from the origin (that is, $\rho = 1/2$). This formula for the contact number follows from the consideration that $\Lambda/f(\Lambda)$ has $\left(t^{1/2}\right)^n = t^{n/2}$ equivalence classes, precisely one of which contains the origin. It is easy to see that

$$c(t,n) = \begin{cases} 1 & t>4 \\ 2 & t=4 \\ 3 & t=3 \\ 2n & t=2 \end{cases}.$$

The case $t=4$ represents an antipodal pair of minimal vectors; the case $t=3$ represents a regular triangle of minimal vectors centered at the origin; and the case $t=2$ represents a regular orthoplex (Conway's nomenclature) or cross-polytope (Coxeter's nomenclature from [11]) of minimal vectors centered at the origin. This formula for $c(t,n)$ follows from the work of [22] which provides a bound on spherical codes, and is discussed in [24], chapter 1. Consequently, for a t-tight lattice,

$$\tau = \begin{cases} t^{n/2}-1 & t>4 \\ 2(4^{n/2}-1) & t=4 \\ 3(3^{n/2}-1) & t=3 \\ 2n(2^{n/2}-1) & t=2 \end{cases}.$$

All of these functions dominate the best upper bounds for contact numbers in large enough dimensions; see [24], chapter 1, which reports the Kabatiansky-Levenshtein upper bound of $2^{0.401n(1+o(1))}$ [14]. Consequently, tight lattices exist in only a finite number of dimensions. Also, the contact number formula implies that if t is not a perfect square, n must be even. Figure 8 illustrates the contact number functions described above, as well as the best known contact numbers for lattices and the best known upper bound on lattice contact numbers; the last two items are taken from [24] (chapter 1) and the preface to the third edition, and from [30]. In the chart, tau$t$ stands for the contact numbers for a t-tight lattice.

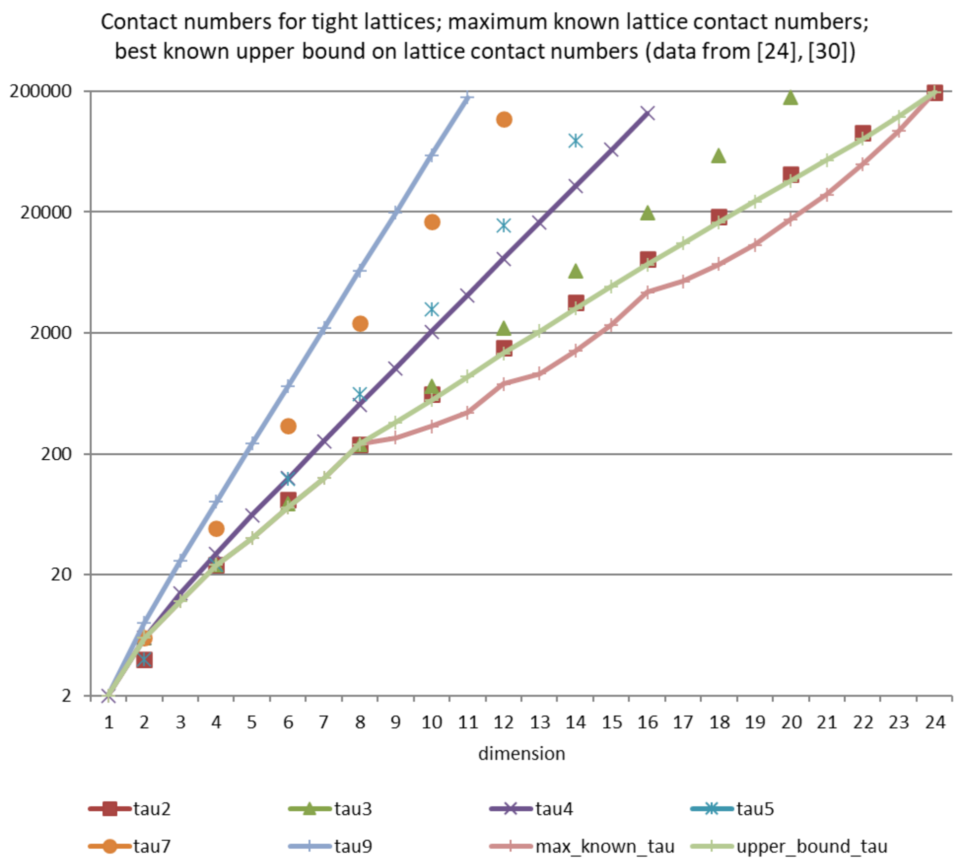

Figure 8. *Contact numbers for tight lattices.*

Further, Λ is *"holey" t-tight* if it is t-tight for some t as above, and for every minimal vector v, $f^{-1}(v)$ is a deep hole near the origin that witnesses the t-tightness of Λ, in the sense of being the center of a Delaunay cell having $c(t,n)$ vertices. When $t<4$, we further assume that $\frac{1}{t}f^2$ is a fixed-point-free automorphism of Λ of period $2t$. Table 19 enumerates the known tight lattices. We conjecture that this list is complete, but have not been able to prove it. (Below, we will establish a partial classification of the tight lattices.) Conway and Sloane proved a theorem that, in our notation, is equivalent to stating that the only 4-tight lattices are $\mathbb{Z}$ and A_2; see [16]. Note too that all known 7-tight and 3-tight lattices are Eisensteinian, and all known 5-tight and 2-tight lattices are Gaussian. This is enough to verify the completeness of the classification of tight lattices in less than 4 dimensions.

Table 19. *Known tight lattices.*

Dimension	Name (up to similarity)	9-tight	7-tight	5-tight	4-tight	3-tight	2-tight	Holey 4-tight	Holey 3-tight	Holey 2-tight
1	$\mathbb{Z}$	✓			✓			✓		
2	A_2		✓		✓	✓			✓	
2	$\mathbb{Z}^2$			✓			✓			✓
4	D_4			✓		✓	✓			✓
8	E_8					✓	✓			✓
24	Λ_{24}, the Leech lattice						✓			✓

The tightness of the 1-dimensional and 2-dimensional lattices listed above is illustrated in figure 9.

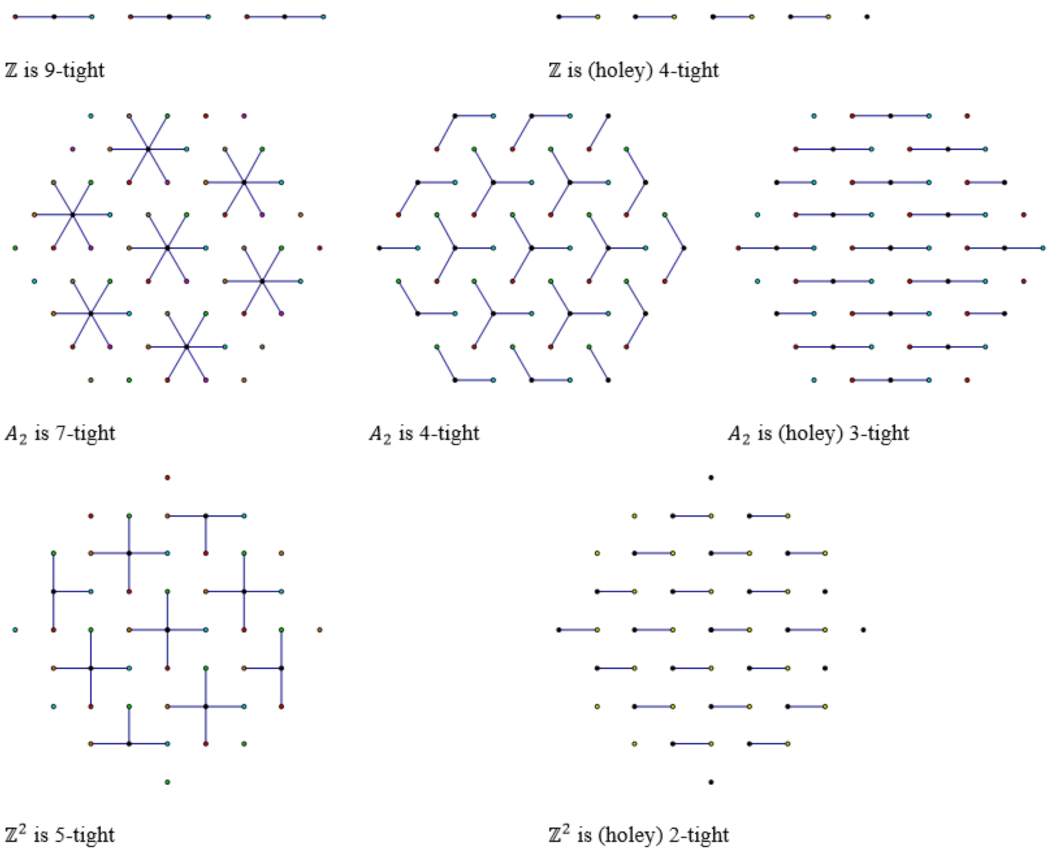

Figure 9. *The tightness of $\mathbb{Z}$, A_2, and $\mathbb{Z}^2$.*

If we could see them in their higher dimensions, corresponding diagrams for the other tight lattices would be illustrated as follows. The 5-, 3-, and 2-tightness of D_4 will be described by considering the latter as the underlying lattice of the Hurwitz integers, H.

The 5-tightness of D_4 is illustrated by connecting 0 to the 24 units of H, and then translating this diagram by multiples of $2+i$;

The 3-tightness of D_4 is illustrated by connecting 0 to ±1, ±*i*, ±*j*, and ±*k*, and then translating this diagram by multiples of $\frac{3}{2}+\frac{1}{2}(i+j+k)$;

The 2-tightness of D_4 is illustrated by connecting 0 to 1 and $-\frac{1}{2}\pm\frac{1}{2}(i+j+k)$, and then translating this diagram by multiples of $1+i$.

The 3- and 2-tightness of E_8 will be described by considering the latter as the underlying lattice of the Dickson integers, D; for more on which, see [21].

The 3-tightness of E_8 is illustrated by connecting 0 to 80 of the units of D, forming the vertices of a certain regular quaternionic polygon described first in [12] and in more detail in [9] (see the enumeration of the roots of the root system P_1 in [9], a sequel to [8]), and then translating this diagram by multiples of a Dickson integer of norm 3;

The 2-tightness of E_8 is illustrated by connecting 0 to $2^4-1=15$ of the units of D, such as 1 and the 14 vectors $\frac{1}{2}\pm\frac{1}{2}(i_n+i_{n+1}+i_{n+3})$ for n a member of $\mathbb{Z}/(7)$, and then translating this diagram by multiples of a Dickson integer of norm 2, such as $\frac{1}{2}+\frac{1}{2}\sum_{n=0}^{6} i_n$.[xxvi]

The 2-tightness of Λ_{24} is illustrated by connecting the origin to $2^{12}-1=4095$ minimal vectors, and then translating this diagram by multiples of a norm 8 vector.

The following theorem partially settles the classification of holey tight lattices.

Theorem. The only holey t-tight lattices for $t>2$ are the ones shown in table 17. That is, no lattice is holey t-tight for $t>4$; only $\mathbb{Z}$ is holey 4-tight; and only A_2 is holey 3-tight. Furthermore, the only holey 2-tight lattices in fewer than 26 dimensions are $\mathbb{Z}^2$, D_4, E_8, and Λ_{24}.

Proof. Let d_1 be the distance from the origin to a minimal vector, so $d_1=2\rho$, or $\rho=d_1/2$. f^{-1} divides distances by $\sqrt{t}$, so by definition of holey tightness, the distance between the origin and the closest deep hole is the covering radius $R=d_1/\sqrt{t}$. The covering ratio R/ρ is therefore $(d_1/\sqrt{t})/(d_1/2)=2/\sqrt{t}=\sqrt{4/t}$. Because by definition the covering ratio must always be at least 1, t can never exceed 4. If $t=4$, then the covering ratio is 1, and the only lattice whose covering radius equals its packing radius is $\mathbb{Z}$ (this conclusion also follows from the bound discussed below).

We can appeal to a Rogers-type argument (see [23, 6]) to conclude that the covering ratio for an n-dimensional lattice must always be at least $\sqrt{2n/(n+1)}$. This corresponds to an arrangement of $n+1$ isometric balls, centered on the $n+1$ vertices of an n-dimensional regular simplex of edge length 2. If the radius of the balls is 1, we have an optimal packing of $n+1$ balls in mutual external contact; and in R^n, no more than $n+1$ balls can be in mutual external contact. If the radius of the balls is $\sqrt{2n/(n+1)}$, we have an optimal covering of an open neighborhood of the centroid of the simplex; and in R^n, at least $n+1$ balls are required to cover an open neighborhood of any point. The function $\sqrt{2n/(n+1)}$ is an increasing function of n, increasing asymptotically to $\sqrt{2}$ as n increases without bound.[xxvii]

Substituting $n=2$, we see that the covering ratio for a 2-dimensional lattice must be at least $\sqrt{4/3}$. The only lattice with this covering ratio must have a Delaunay tessellation by regular triangles; this lattice is therefore A_2. When $n>2$, the covering ratio must be at least $\sqrt{6/4}=\sqrt{3/2}$, which is greater than $\sqrt{4/3}$. Thus the enumeration of holey t-tight lattices for $t>2$ is complete.

From the computation above, a holey 2-tight lattice must have covering ratio $\sqrt{2}$. If Λ is holey 2-tight and n-dimensional, f is as in the definition of holey 2-tightness, and v is a minimal vector of Λ, then $f^{-1}(v)$ is the center of a deep hole of type A_1^n, a regular orthoplex or cross-polytope. The vectors along the edges of this deep hole generate a sublattice of Λ of type D_n. Thus, a subset of the minimal vectors of Λ generate a copy of D_n; alternatively, we may say that Λ consists of a union of D_n together with (a possibly empty set of) translates of the latter.

We now consider the low-dimensional cases. $D_2\sim\mathbb{Z}^2$ (at different minimal norms), so in the cases of D_2 and D_4, no additional translates are needed (or possible without diminishing the minimal norm), and these two lattices are holey 2-tight. The covering ratio of D_n is $\sqrt{n/2}$ when $n\geq 4$; see [24], chapter 4. One can add translates to a lattice without diminishing its minimal norm if and only if the covering ratio is at least 2. The covering ratio of D_6 is $\sqrt{3}$, so it is not possible to add translates to it without diminishing its minimal norm; yet it is not holey 2-tight, as its covering ratio is not $\sqrt{2}$. The covering ratio of D_8, on the other hand, is exactly $\sqrt{4}=2$, so it is possible to add translates to this lattice without diminishing its minimal norm. The deep holes of D_8 are isometric (although there are two equivalence classes of deep holes under translations of the lattice), so we may adjoin a new lattice vector precisely at the center of a deep hole, and only at such a point. The resulting lattice is E_8, which is holey 2-tight.

From 10 to 24 dimensions, we may narrow down our search rapidly by computing values of the contact number $\tau=2n(2^{n/2}-1)$ as n varies over even numbers from 10 to 24. Most of the values so computed exceed the upper bounds on contact numbers enumerated in [24] (chapter 1) and [30], and thus are impossible to achieve. The only interesting cases are in 16 and 24 dimensions.

In 16 dimensions, the contact number of a 2-tight lattice would be 8160. This is less than the upper bound reported in [24], chapter 1, for a lattice packing (8312), but nearly double the contact number of the current highest packing number for 16 dimensions (4320), achieved by Λ_{16}. Such a lattice packing has now been ruled out by the results in [30], where the authors establish 7320 as an upper bound for the contact number in 16 dimensions.

In 24 dimensions, the contact number of a 2-tight lattice is 196560. It is shown by Bannai and Sloane in [24], chapter 14 (relying on an argument by Conway in [24], chapter 12) that such a local arrangement is unique; indeed the lattice is similar to the Leech lattice.

Thus the only open cases in the classification of holey tight lattices are regarding the existence of 2-tight lattices in even dimensions greater than 24. We can now say definitively that the only holey tight lattices in no more than 24 dimensions are $\mathbb{Z}$, A_2, $\mathbb{Z}^2$, D_4, E_8, and Λ_{24}.

The earlier observation about the Eisensteinian structure of the known 3-tight lattices sheds no light on holey 3-tight lattices, where the only case is A_2, the lattice underlying the Eisenstein integers. However, the apparent Gaussian structure of the holey 2-tight lattices is more fruitful for investigation. Let f be as in the definition of holey 2-tight lattices. Then f^2 is also a similarity and endomorphism of Λ. Moreover, $\frac{1}{2}f^2$ is a fixed-point-free isometry of Λ of period 4. This gives Λ the structure of a Gaussian lattice over $\mathbb{Z}[\frac{1}{2}f^2]$. So we can narrow our search for higher dimensional holey tight lattices to Gaussian lattices.

For the first five of the holey tight lattices listed above ($\mathbb{Z}$, A_2, $\mathbb{Z}^2$, D_4, and E_8), the unique value of t for which each is holey t-tight is equal to the value of the shape parameter for that lattice.

9. Dimensions

When discussing these exceptionally well-behaved lattices, I have been asked what makes them - or the dimensions in which they appear - so special. With the identification of holey tightness, we can answer the question about the lattices. More can be said about the lattices, however, incorporating the status of all of them as low-dimensional laminated lattices over appropriate Euclidean rings of integers, or as the lattice underlying these rings of integers themselves.

Consider the regular simplex α_n and the regular orthoplex (or cross-polytope) β_n. At edge length $\sqrt{2}$, the edges of these two polytopes generate, respectively, the root lattices A_n and D_n. We are interested in a special case of commensurability[xxviii] between these two root lattices. Choose coordinates so that the vertices of β_n are $(\pm 1,0,\ldots,0)^S$ (where the superscript means that all coordinate permutations are allowed). We now construct an α_n exterior to β_n in the positive orthant, such that the intersection of the two polytopes is the α_{n-1} with vertices $(1,0,\ldots,0)^S$. It is not difficult to show that the remote vertex of the α_n just constructed is $\left(\frac{1}{k},\ldots,\frac{1}{k}\right)$, where $k=\sqrt{n+1}-1$. Therefore, in this position, A_n and D_n are commensurable provided n is one less than a perfect square. When $n=k(k+2)$, the lattice generated by the union of A_n and D_n is integral at minimal norm $lcm(2,k)$. This sheds light on the cases $k=1$, where $A_3 \cong D_3$; $k=2$, where the union of A_8 and D_8 generate E_8; and $k=4$, where A_{24} and D_{24} are Niemeier lattices commensurable with the Leech lattice.

10. Summary

Nearly every lattice mentioned in the section on conjectures, namely, the known Coxeter-celled lattices, the known lattices with large shape parameter, the known 2-pretty lattices, the known prompt lattices, and the known tight lattices, are all either sections or projections of the Leech lattice (when appropriately scaled), often both, lending more support for the universality of the Leech lattice, should the conjectures prove correct. Most of the lattices mentioned in these classifications are miniature versions of the Leech lattice, in the sense that not only are they sections or projections of the Leech lattice and have automorphism groups contained within Co_0, but they are themselves integral lattices, similar to their duals using an endomorphism-similarity multiplying all norms by a small natural number, typically 1, 2, or 3. Lattices of that sort are unimodular, 2-modular, or 3-modular respectively, and are classified in [5]. Indeed, more is true; the lattices in question are self-dual over appropriate rings of integers. If the conjectures of this paper prove correct, then understanding the Leech lattice as a whole can be approached through the understanding of the lattices $\mathbb{Z}$, A_2, $\mathbb{Z}^2$, D_4, E_8, K_{12}, and Λ_{16}, as well as the cellular structure of the Leech lattice elucidated in this paper.

Acknowledgments

The author wants to thank John Conway and Neil Sloane for many stimulating conversations about lattices over the years. After the works of H. S. M. Coxeter, Conway's and Sloane's book *Sphere Packings, Lattices and Groups* has done the most to refocus the author's mathematical interests. Thanks to Conway's teaching him the "starry" coordinate system, the author feels more comfortable travelling in R^{24}; this paper fulfills the author's wish to map R^{24} and to make the Leech lattice visible and more familiar.

Most importantly, the author thanks his wife Yan for her boundless encouragement and patience over the years.

"…Behold, he stands behind our wall, gazing in at the windows, looking through the lattices."

Song of Songs 2: 9

Author Contributions

Hal M. Switkay is the sole author. The author read and approved the final manuscript.

Statements and Declarations

No fund, grant, or other support was received. The author has no financial or non-financial interest to disclose. We do not analyze or generate any datasets, because our work proceeds within a theoretical and mathematical approach.

Conflicts of Interest

The author declares no conflicts of interest.

References

[1] Conway, J. H., Curtis, R. T., Norton, S. P., Parker, R. A., Wilson, R. A. Wilson: *ATLAS of Finite Groups*, Oxford University Press, 1985.

[2] BBC. The Museum of Curiosity. Available from: http://www.bbc.co.uk/radio4/comedy/museumofcuriosity_gallery_20080319.shtml (accessed 16 July 2025).

[3] Borcherds, R. E.: *The Leech lattice*, Proceedings of the Royal Society A *398*(1985), 365-376.

[4] Borcherds, R. E.: *Lattices like the Leech lattice*, Journal of Algebra *130*(1990), 219-234.

[5] Nebe, G., Sloane, N. J. A.: *A Catalogue of Lattices*, http://www.math.rwth-aachen.de/~Gabriele.Nebe/LATTICES/

[6] Coxeter, H. S. M., Few, L., Rogers, C. A.: *Covering space with equal spheres*, Mathematika *6*(1959), 147-157.

[7] Conway, J. H., Sloane, N. J. A.: *Complex and integral laminated lattices*, Transactions of the American Mathematical Society *280*(1983), 463-490.

[8] Cohen, A. M.: *Finite complex reflection groups*, Annales Scientifiques de l'École Normale Supérieure *9*(1976), 379-436.

[9] Cohen, A. M.: *Finite quaternionic reflection groups*, Journal of Algebra *64*(1980), 293-324.

[10] Conway, J. H.: private communication.

[11] Coxeter, H. S. M.: *Regular Polytopes*, Dover, 3rd edition, 1973.

[12] Crowe, D. W.: *A regular quaternion polygon*, Canadian Mathematical Bulletin *2*(1959), 77-79.

[13] du Sautoy, M.: *Symmetry: A Journey into the Patterns of Nature*, Harper, 2008.

[14] Kabatiansky, G. A., Levenshtein, V. I.: *Bounds for packings on a sphere and in space*, Problems of Information Transmission *14*(No. 1, 1978), 1-17.

[15] Conway, J. H., Sloane, N. J. A.: *Low-dimensional lattices V: Integral coordinates for integral lattices*, Proceedings of the Royal Society A *426*(1989), 211-232.

[16] Conway, J. H., Sloane, N. J. A.: *Low-dimensional lattices VI: Voronoi reduction of three-dimensional lattices*, Proceedings of the Royal Society A *436*(1991), 55-68.

[17] University of California at Santa Barbara. Exceptional Mathematics. Available from: https://web.math.ucsb.edu/~jon.mccammond/math/ex.html (accessed 16 July 2025).

[18] Nebe, G.: *An even unimodular 72-dimensional lattice of minimum 8*: https://arxiv.org/abs/1008.2862

[19] The Online Encyclopedia of Integer Sequences, A330586: https://oeis.org/A330586

[20] Switkay, H. M.: *The Periodic Table of Numbers* (unpublished).

[21] Conway, J. H., Smith, D. A.: *On Quaternions and Octonions: Their Geometry, Arithmetic, and Symmetry*, Peters, 2003.

[22] Rankin, R. A.: *The closest packing of spherical caps in n dimensions*, Proceedings of the Glasgow Mathematical Association *2*(1955), 139-144.

[23] Rogers, C. A.: *The packing of equal spheres*, Proceedings of the London Mathematical Society *8*(1958), 609-620.

[24] Conway, J. H., Sloane, N. J. A.: *Sphere Packings, Lattices and Groups*, 3rd edition, Springer-Verlag, 1999.

[25] Schürmann, A., Vallentin, F.: *Computational Approaches to Lattice Packing and Covering Problems*, Discrete and Computational Geometry *35*(2006), 73-116.

[26] Schürmann, A., Vallentin, F.: *Local Covering Optimality of Lattices: Leech Lattice versus Root Lattice E_8*, International Mathematics Research Notices *32*(2005), 1937-1955.

[27] Thompson, J. G.: *Finite groups and even lattices*, Journal of Algebra *38*(1976), 523-524.

[28] Thompson, T. M.: *From Error-Correcting Codes through Sphere Packings to Simple Groups*, Mathematical Association of America, 1983.

[29] Tits, J.: *Quaternions over $Q[\sqrt{5}]$, Leech's lattice and the sporadic group of Hall-Janko*, Journal of Algebra *63*(1980), 56-75.

[30] Leijenhorst, N., De Laat, D.: *Solving Clustered Low-Rank Semidefinite Programs Arising from Polynomial Optimization*: https://www.arxiv.org/abs/2202.1207

i In the section on conjectures, we discuss very strong properties enjoyed by only a finite number of lattices, the largest of which are E_8 and Λ_{24}. We note further that E_8 and Λ_{24} are the first self-dual lattices at minimal norms 2 and 4 respectively (see [24], chapter 7); the icosian ring $\mathbb{Z}[2Alt_5]$ has a norm under which it appears as E_8, and the first non-trivial self-dual lattice over the icosians is the Leech lattice (see [24], chapter 8); and the lowest dimensional irreducible, globally irreducible lattices are $\mathbb{Z}$, E_8, and Λ_{24} (a lattice Λ is globally irreducible if $\Lambda/p\Lambda$ is irreducible for all primes *p*; see [27]).

ii Jon McCammond has a webpage giving a bare outline of exceptional mathematics, and a few links [17].

iii An E_8^3-based Turyn-type construction is given for the Leech lattice in [24], chapter 8. However, this algebraic construction does not bear on the more geometric concerns of this paper.

iv The reader needs to be familiar with at least the A-D-E type Coxeter-Dynkin diagrams. They are displayed in [24], chapters 4 and 23. The weights are described in [11], chapter 11, and in [24], chapter 23.

v We thank an anonymous reviewer for bringing to our attention an alternative formulation of the total weight product (twp). Each connected Coxeter-Dynkin diagram X_n has other numbers associated with it: the order of the reflection group $W = |W(X_n)|$, and the order of the dual quotient group $|G_\infty|$. The order of the dual quotient group is $n+1$ for A_n, 4 for D_n, 3 for E_6, 2 for E_7, and 1 for E_8. For each connected Coxeter-Dynkin diagram of rank *n*:

$$twp = W/(|G_\infty| \times n!)$$

vi The pointwise stabilizer of a minimal 4-dimensional regular simplex within the Leech lattice - that is, a graph of the form a_1^5 - is the group $2^5{:}M_{20} \cong 2^5{:}(2^4{:}Alt_5)$ of order 30720. It has two orbits of vectors at minimal distance from the original five vectors, one of size 10 and one of size 160; see [28].

vii This infinite graph, which we dub the Leech graph, can be seen as the Coxeter-Dynkin diagram of a reflection group with generators of order 2 corresponding to each vector in the Leech lattice, with generators commuting if they are not joined, and products of generators having order 3 if they are singly-joined. The resulting reflection group acts in 26-dimensional Lorentzian space (that is, $R^{25,1}$) or in 25-dimensional real hyperbolic space; see [24], chapter 27, and [3].

viii Most of the figures in this paper were created using Geometer's Sketchpad.

ix The claim about the volume of the deep holes and the shallow holes in the vicinity of E_8^3 can be verified as follows. For each such hole (for example the holes in the table of neighbors of E_8^3), compute svol/g, the popularity of the hole, based on the statistics given in [24], chapter 25. The sum of the popularities of these holes is more than 90% of $74613 = 24!/|Co_0|$, the sum over all holes.

x In all of the diagrams $X+n$ in figure 2, vectors that happen to belong to the original E_8^3+3 are shown uniformly in their "proper" positions. However, vectors of $X+n$ whose magnitudes with respect to the original E_8^3 are greater than 3 are shown in different positions in different diagrams, with the goal of increasing the legibility of the individual diagrams. This makes identification and comparison between different diagrams more difficult. The difficulty is eased by determining the coordinates of the vectors with respect to the original E_8^3.

xi Conway observed [10] that the E_8 diagram has been given another labeling that is useful for group theorists. The nodes along the spine may be called 1A, 2A, 3A, 4A, 5A, 6A, 4B, 2B, with the additional node called 3C. These are the names of conjugacy classes within the Monster simple group. Such considerations are of interest for group theorists, but are not needed for the geometrical goals of this paper.

xii There is a curious feature of the labels' positions in figure 3, which may be seen as a Coxeter-Dynkin diagram for a reflection group: $Aut_\infty(E_8)$, the full automorphism group of the E_8 lattice, including translations. Each node corresponds to a reflection in a (7-dimensional) hyperplane within R^8. Nodes not connected directly by an edge correspond to perpendicular hyperplanes, and thus the reflections commute; while nodes connected directly by an edge correspond to hyperplanes meeting at an angle of $\pi/3$, and thus the product of reflections in these hyperplanes has period 3. This much is true of any Coxeter-Dynkin diagram. But since the E_8 diagram is a tree, its nodes may be partitioned into two disjoint classes of disconnected nodes: {e8, e6a2, a4a4, a7a1, a8} and {e7a1, d5a3, a5a2a1, d8}. Within each class, all the reflections commute, so the product of all reflections in each class has period 2. These two isometries of period 2 generate a dihedral group of infinite degree, the isometry group of a Petrie apeirogon of the E_8 lattice; see [11]. The diagram displays labels for members of the first class below the nodes, while labels for members of the second class are displayed above the nodes. A similar labeling convention exists for E_7, E_6, D_n, and A_{2n-1}.

xiii An autometry is an isometry from an object onto itself.

xiv Apologies to the King of Siam, Richard Rodgers and Oscar Hammerstein, and Yul Brynner.

xv There are errata to chapter 18 of [24] that affect the computations needed to verify the accuracy of table 4. Specifically, on p. 439 of [24], in paragraph XXII: $R = E_7 + A_{17}$, the statement $l(9) = 2$ should be changed to $l(9) = 9/2$; and in paragraph XXIII: $R = E_6 + D_7 + A_{11}$, the generator described in the last sentence should not be $(1,1)$ but rather $(1,1,1)$.

xvi Chapter 29 of [24] enumerates the weight distribution $(0^1 1^{24} 2^{276} 3^{2024} 4^{1771})$ of the Golay cocode of length 24: that is, the weight distribution of $2^{24}/G_{24}$, where G_{24} is the Golay binary code of length 24. These exponents, multiplied by $4096 = 2^{12}$, yield the number of cells in the respective orbits of neighbors of A_1^{24}. Analogously, by dividing the number of cells in the respective orbits of neighbors of A_2^{12} by $729 = 3^6$, of A_3^8 by $256 = 4^4$, and of A_4^6 by $125 = 5^3$, we discover the weight distribution of other important cocodes: $3^{12}/G_{12}$, where G_{12} is the Golay ternary code of length 12; $4^8/G_8$, where G_8 is the quaternary code of length 8 described by Venkov in [24], chapter 18 (its elements of order 1 and 2 form the well-known Hamming binary code of length 8); and $5^6/G_6$, where G_6 is the quinary code of length 6 also described by Venkov. The corresponding weight distributions are $0^1 1^{24} 2^{264} 3^{440}$, $0^1 1^{16+8} 2^{112+112+7}$, and $0^1 1^{12+12} 2^{60+40}$. The weight distribution of the cocode of the hexacode of length 6 over the field of 4 elements is $0^1 1^{18} 2^{45}$, corresponding to the first three orbits of neighbors of D_4^6. Extensions of table 6 to other deep holes would yield information about other smaller cocodes.

xvii Among the neighbors of D_4^6 are other copies of D_4^6. This may help to explain a cryptic remark at the end of [24], chapter 25: "If the closed polytopes corresponding to the deep holes of type D_4^6 are deleted from R^{24}, the resulting space is disconnected." This claim is not proved in [24]. If true, however, such an argument must presumably apply as well to the deep holes of type E_8^3. Let us call a deep hole *X ubiquitous* if the elimination of the closed polytopes of type *X* from R^{24} disconnects the space. This raises a question: which deep holes are ubiquitous?

xviii An anonymous reviewer notes that theta series in general are determined by finite initial segments. This does not imply our stronger conjecture, that the necessary initial segment is determined by twice the generating norm.

xix Along these lines, an anonymous reviewer points out the existence of a much-better known $\mathbb{Z}$-module of rank $\varphi(m)$ with an automorphism of order *m*, namely $\mathbb{Z}[\omega_m]$, where ω_m is a primitive *m*-th root of unity. This ring is dense in $\mathbb{C}$ when $\varphi(m) > 2$. The issue arises as to the structure of this lattice when given a Euclidean norm, if this can be done in a canonical fashion. We do not know if this lattice would be similar to L_m.

xx Conway and Sloane observe that this corollary is itself a powerful generalization of Lagrange's four-square theorem.

xxi The Periodic Table of Numbers displays the natural numbers. It is designed with luminosity = 0 for the number 1; luminosity increases for increasing numbers. Hue is arbitrarily chosen as red for powers of 2; the hue of any number multiplied by a power of 2 equals the hue of the original number. This coloring scheme was originally designed to provide a colorful notation system for musical harmonics, in which tones separated by a whole number of octaves (and thus frequencies whose ratio is an integral power of 2) have the same musical color, and are said to belong to the same tone class.

xxii An anonymous reviewer observes that we would consider Z^n to be *n*-pretty, were it not for the fact that the automorphism group of the lattice must act transitively on the non-empty set of regular simplexes of *n* minimal vectors at minimal distance from each other, and the integer lattice lacks such minimal regular simplexes in more than 1 dimension.

xxiii An anonymous reviewer has identified a counterexample to the conjecture in this sentence. The 3-dimensional lattice is generated by orthogonal vectors *u*, *v*, and *w*, of respective norms 2, 3, and 4. This lattice has reach 6, because there are two distinct orbits of vectors of norm 12 that are inequivalent under the symmetry group 2^3, namely $2u + w$ and $2v$. This example, however, remains consistent with the observation that even for the most symmetrical lattices, reach decreases as dimension increases. We seek a provable upper bound on reach as a function of dimension.

xxiv We use $\mathbb{Z}$ to stand for the ring of real rational integers as well as for the 1-dimensional lattice. There are two discrete cyclotomic properly complex rings, both of which are Euclidean: $\mathcal{G} = \mathbb{Z}[C_4]$, the Gaussian integers, whose underlying lattice is $\mathbb{Z}^2$; and $\mathcal{E} = \mathbb{Z}[C_6]$, the Eisensteinian integers, whose underlying lattice is A_2. There are two discrete cyclotomic properly quaternionic rings that are Euclidean: $\mathcal{F} = \mathbb{Z}[Q_3]$, whose underlying lattice is A_2^2, and generated by the binary dihedral group of order 12; and $\mathcal{H} = \mathbb{Z}[2Alt_4]$, the Hurwitzian integers, whose underlying lattice is D_4, and generated by the binary tetrahedral group. These two rings both include the previous two rings. Lastly, there is a unique discrete cyclotomic properly octonionic ring that is Euclidean, namely, $\mathcal{D}$, the integral octonions of Dickson, which contains the previously mentioned rings, and whose

underlying lattice is E_8.
Now we employ the notation of [7]; the latter paper extends the notion of laminated lattices (see [24], chapter 6) to complex and quaternionic rings. The densest 2-dimensional lattice over a Euclidean ring $\mathcal{J}$ is necessarily $\Lambda_{2,\mathcal{J}}$. Then $\Lambda_{2,Z}$ is A_2; $\Lambda_{2,\mathcal{G}}$ and $\Lambda_{2,\mathcal{E}}$ are both D_4 (while taking $\mathcal{K}$ to be the Kleinian integers, $\Lambda_{2,\mathcal{K}}$ is A_2^2); $\Lambda_{2,\mathcal{F}}$ and $\Lambda_{2,\mathcal{H}}$ are both E_8. We cannot define modules over the non-associative ring of integral octonions, but substituting the dense cyclotomic quaternionic ring of icosians $\mathcal{I} = \mathbb{Z}[2Alt_5]$ generated by the double cover of the alternating group of degree 5 (the binary icosahedral group), which under an appropriate norm appears as E_8 (see [24], chapter 8), $\Lambda_{3,\mathcal{I}}$ is the Leech lattice.
While on the subject of complex and quaternionic lattices, we note the great importance of the first self-dual lattice, at minimal norm 2, over $\mathbb{Z}$ as well as $\mathcal{G}$ is E_8; over $\mathcal{E}$ as well as $\mathcal{F}$ is the Coxeter-Todd lattice K_{12}; over $\mathcal{H}$ is the Barnes-Wall lattice $\Lambda_{16} = \Lambda_{4,\mathcal{H}} = \Lambda_{2,\mathcal{I}}$; and over $\mathcal{I}$ is the Leech lattice. These prompt lattices were identified earlier. K_{12} and Λ_{16}, despite their importance, do not figure prominently in this paper because their covering ratios, $\sqrt{8/3}$ and $\sqrt{3}$ respectively, are larger than $\sqrt{2}$, and thus their Delaunay cells cannot be described by Coxeter-Dynkin diagrams of A-D-E type, that is to say they are not Coxeter-celled as defined above; however see [4], who describes deep holes of these lattices to be of types G_2^6 and F_4^4 respectively.

[xxv] Such a structure may well exist. Let λ be a root of $x^2 \pm x + 2 = 0$; then $\mathcal{K} = \mathbb{Z}[\lambda]$ forms the Kleinian integers. The vectors $(2,0,0)$, $(\lambda,\lambda,0)$, and $(\bar{\lambda},1,1)$ generate a 3-dimensional Kleinian lattice M_3 (self-dual at minimal norm 2), which is closed under vector products of the form $u \times \bar{v}$ at large enough minimal norm. Tensored up to the quaternionic ring $\mathcal{F}$, the real version of $M_3 \otimes_{\mathcal{K}} \mathcal{F}$ is the Coxeter-Todd lattice K_{12}; tensoring further to the icosian ring $\mathcal{I}$, the real version of $M_3 \otimes_{\mathcal{K}} \mathcal{I} = M_3 \otimes_{\mathcal{F}} \mathcal{I}$ is the Leech lattice.
These observations lead to a fascinating relationship between E_8 and the Leech lattice, which the author calls "the great isomorphism". Let $\mathcal{J}$ stand for one of the nested series of rings $\mathcal{K} \subset \mathcal{F} \subset \mathcal{I}$. E_8 can be seen as a 4-, 2-, or 1-dimensional lattice over these respective rings, whose respective automorphism groups have the form $2\mathrm{Alt}_n$, where n = 7, 6, or 5 respectively. The centralizers of these groups within Co_0 are $2L_3(2)$, $2U_3(3)$, and $2J_2$ respectively, each of which is respectively isomorphic, miraculously, to the automorphism group of $M_3 \otimes_{\mathcal{K}} \mathcal{J}$ as a 3-dimensional $\mathcal{J}$-lattice for the appropriate $\mathcal{J}$. In other words:

$$\mathrm{Cent}(\mathrm{Aut}(\Lambda_{24}),\mathrm{Aut}_{\mathcal{J}}(E_8)) \cong \mathrm{Aut}_{\mathcal{J}}(M_3 \otimes_{\mathcal{K}} \mathcal{J})$$

This isomorphism deserves an explanation.

[xxvi] We employ a definition of the real octonion algebra O as being spanned over R by the eight units $i_\infty = 1$, and i_n, where n is a member of $\mathbb{Z}/(7)$. For every such n, i_∞, i_n, i_{n+1}, and i_{n+3} span a real quaternion algebra H. This determines all possible products of units, hence all multiplication within O. This construction displays the embedding of $L_3(2)$ in $\mathrm{Aut}(\mathcal{D})$.

[xxvii] This explains the interest in the few lattices in more than 3 dimensions with covering ratio no more than $\sqrt{2}$. In fact, stronger lower bounds on the covering ratio are known now, thanks to stronger upper bounds on the packing radius; see [24], chapters 1 and 2. Consequently, lattices with covering ratio no more than $\sqrt{2}$ only exist in a finite number of dimensions. Every such lattice known to the author in more than 3 dimensions is Coxeter-celled.

[xxviii] Recall that lattices A and B are commensurable provided that their intersection has finite index in each of them; equivalently, the union of A and B generates a (discrete) lattice; equivalently, $A \subset \mathbb{Q} \otimes B$ and $B \subset \mathbb{Q} \otimes A$.